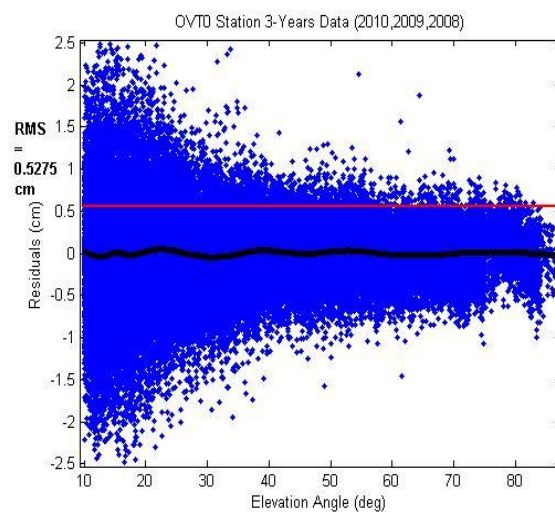


CHALMERS



Evaluation of SWEPOS Second-Order GNSS Network Stations for Monitoring Tropospheric Water Vapor

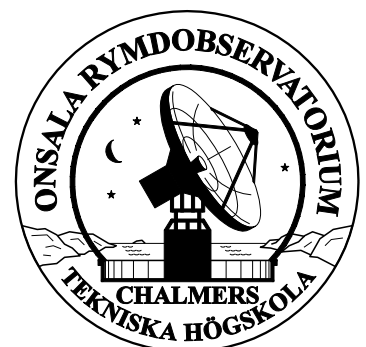
Muhammad Tariq Aziz

Department of Earth and Space Sciences

Space Geodesy and Geodynamics Group

CHALMERS UNIVERSITY OF TECHNOLOGY

Gothenburg, Sweden, 2011



Thesis for the Degree of Master of Science

Evaluation of SWEPOS Second-Order GNSS Network Stations for Monitoring Tropospheric Water Vapor

Muhammad Tariq Aziz



CHALMERS

Department of Earth and Space Sciences
Space Geodesy and Geodynamics Group
CHALMERS UNIVERSITY OF TECHNOLOGY
Gothenburg, Sweden, 2011

Evaluation of SWEPOS Second-Order GNSS Network Stations for Monitoring Tropospheric Water Vapor

Muhammad Tariq Aziz

Supervisor:

Dr. Jan M. Johansson

Adjunct Professor

Space Geodesy and Geodynamics Group

Department of Earth and Space Sciences

Chalmers University of Technology

© Muhammad Tariq Aziz, 2011.

Department of Earth and Space Sciences

Chalmers University of Technology

SE-412 96 Gothenburg, Sweden

Telephone +46 (0)31-772 10 00

www.chalmers.se

Cover:

The pictures on the title page are of SWEPOS second-order Gryt station (left) which is built on the roof top surrounded by some pillar and other antenna and Residual plot (right) as an angle of Elevation angle (blue dots) including red line show the root mean square and black line is the trend of the Övertorneå station. The residual plot is plot over the period of last three year from 2008 to 2011. Here the root mean square is around 0.5cm with 10 degree elevation cut-off angle. The plot has been made of the data that was processed through GIPSY which based on the precise positioning technique.

Evaluation of SWEPOS Second-Order GNSS Network Stations for Monitoring Tropospheric Water Vapor

©Muhammad Tariq Aziz

Department of Earth and Space Sciences

Chalmers University of Technology

Gothenburg, Sweden 201

Abstract

Global Navigation Satellite Systems (GNSS) are used in many applications demanding millimeter level accuracy in positioning. These applications includes land monitoring, crustal movements, detection of large co-seismic displacements

Water vapor is widely recognized to be of fundamental importance in determining climate and its sensitivity.

Thesis work primarily focus on the assessment of the signal propagation delay estimates from GNSS by comparison with independent data sets such as measurements from climate models and other GNSS processing. This study compares Satellite measurement with other climate models for the period of 2008 - 2011.

This is the first time the second order GNSS stations of SWEPOS had been studied for the Tropospheric delay. For the Nine second-order GNSS station of SWEPOS in Sweden were selected randomly to analyzing water vapor activity. The study is necessary for the Tropospheric region due to all the weather related activity occurs in this region as this region contains more than 90% water vapor.

My Master Thesis project focused on evaluating the use of GNSS data from the SWEPOS network to estimate trends in Zenith Tropospheric Delay (ZTD) and their respective ZWD and ZHD, caused by the presence of atmospheric water vapor. The Swedish permanent GNSS network, SWEPOS, today consists of more than 200 stations. The 25 core stations built on solid rock base with a good electromagnetic environment. SWEPOS have been thoroughly evaluated for this purpose for many years but the more recently installed second-order stations, often built on roof-tops, may also be of interest for Atmospheric monitoring as well as Geophysical projects.

Keywords:

SWEPOS, GNSS, SP, Climate, Second-order, Geodetic, Stations, ZTD, ZWD, ZHD, Tropospheric Water Vapor, Residuals, Wet Delay, Hydrostatic Delay

Acknowledgements

I take immense pleasure in thanking my helpful Supervisor, Professor Dr. Jan M Johansson for believing in me and giving me the opportunity to work in this research and extend my knowledge in GNSS and its applications. The supervision and support that you gave me throughout the thesis, truly helps in the progression and smoothness of this Master Thesis. The cooperation is much indeed appreciated.

My grateful thanks to Tong Ning and all those in the Earth and Space Sciences Department whom I met during Master Thesis, my friends and family members and all those who support me during my thesis.

At the end I would like to thanks one of the wonderful gifts of my life, My Parents, for their uncountable support in every part of my life.

Tariq

Gothenburg, December 2011

List of Acronyms or Abbreviations

BD2 Beidou-2

CDMA Code Division Multiple Access

CME Coronal Mass Ejection

DGPS Differential Global Positioning System

DOP Dilution of Precision

ESA European Space Agency

FDMA Frequency Division Multiple Access

GEO Geosynchronous Earth Orbit

GIPSY/OASIS II GPS Inferred Positioning SYstem and Orbit Analysis SImulation Software

GLONASS Globalnaya Navigatsionnaya Sputnikovaya Sistema (in Russian)

GNSS Global Navigation Satellite System

GPS Global Positioning System

IGS International GNSS Service

JPL Jet Propulsion Laboratory

LEO Low Earth Orbit

MEO Medium Earth Orbit

PPP Precise-Point Positioning

RTK Real Time Kinematics

SWEPOS SWEdish POsitioning System

TEC Total Electron Content

ZHD Zenith Hydrostatic Delay

ZTD Zenith Total Delay

ZWD Zenith Wet Delay

Contents

1	Introduction.....	1
1.1	Structure of the Atmosphere	2
1.2	Motivation	3
1.3	Thesis Structure.....	4
2	GNSS – Global Navigation Satellite System Techniques.....	5
2.1	GPS:	8
2.1.1	GPS contribution to understand climate change:	8
2.2	GLONASS:	8
2.3	GALILEO:	8
2.4	COMPASS:.....	8
2.5	Frequency Information.....	9
2.6	GNSS Applications	9
3	Ground Based GNSS Network/GNSS Reference Stations.....	10
3.1	IGS Geodetic Stations	10
3.2	SWEPOS	11
4	Data and Processing	13
4.1	GIPSY/OASIS:	13
4.2	Selected Stations and Motivation	14
4.3	Data Selection and Motivation.....	15
4.4	Chosen Duration and Motivation.....	16
5	Method.....	17
5.1	Fundamental Equations	17
6	Results	19
7	Comparison and Validation with Independent Data sets/ Other Models.....	37
7.1	Climate Models.....	37
7.2	ECMWF	37
7.3	RCA Model.....	37
7.4	Comparison with Climate Models	38
8	Error Sources	44
8.1	Ionosphere Propagation Path Delay.....	44
8.2	Tropospheric Propagation Path Delay.....	45
8.3	Receiver related errors.....	45
8.4	Satellite ephemeris errors.....	45

8.5	Satellite Geometry.....	46
8.6	Satellite Orbit and Clock Errors	46
8.7	Communication Errors	46
8.8	Space Weather Errors.....	47
8.9	Atmospheric Drag.....	47
8.10	Radio Blackouts	47
8.11	Antenna Phase Center variations.....	47
8.12	Multipath Effects	48
8.13	Gaseous Absorption	48
8.14	Site-dependent Effects.....	48
9	Conclusion	49
10	Future Work and Recommendation.....	51
	Bibliography.....	52
	Appendix A:-	54
	List of Tables.....	54
	Appendix B:-	57
	List of Figures.....	57

List of Figures

➤ Figure 1: Atmospheric Layers based on Temperature with respect to Altitude.....	2
➤ Figure 2: Earth Water Cycle causes a big shift in the Troposphere region includes evaporation, condensation, precipitation and infiltration	3
➤ Figure 3: GNSS Segments, Space segment, Control Segment and User Segment.....	6
➤ Figure 4: IGS Worldwide Geodetic Stations (image courtesy igs).....	11
➤ Figure 5: SWEPOS GNSS Stations in Sweden, First-order Station (left) Second-order Station (right), (Images courtesy of SWEPOS, Sweden)	11
➤ Figure 6: SWEPOS Geodetic Station in Sweden (Image courtesy of SWEPOS Sweden)	12
➤ Figure 7: A typical GNSS (GOA-II) software processing.....	13
➤ Figure 8: Selected second-order SWEPOS stations, green pointer on the map (Image courtesy google earth)	15
➤ Figure 9: Älvsbyn station (left), Zenith Tropospheric Delay (right).....	19
➤ Figure 10: Zenith Hydrostatic Delay plot (left) and its corresponding Zenith Wet Delay plot (right).....	19
➤ Figure 11: Älvsbyn station Residual plot as an angle of Elevation angle (left) and as an angle of Azimuth angle (right). Black line is the trend; red line is the root mean square ..	20
➤ Figure 12: Gryt station (left), Zenith Tropospheric Delay (right)	21
➤ Figure 13: Zenith Hydrostatic Delay plot (left) and its corresponding Zenith Wet Delay plot (right).....	21
➤ Figure 14: Gryt station Residual plot as an angle of Elevation angle (left) and as an angle of Azimuth angle (right). Black line is the trend; red line is the root mean square	22
➤ Figure 15: Hisingsbacka station (left), Zenith Tropospheric Delay (right)	23
➤ Figure 16: Zenith Hydrostatic Delay plot (left) and its corresponding Zenith Wet Delay plot (right).....	23
➤ Figure 17: Hisingsbacka station Residual plot as an angle of Elevation angle (left) and as an angle of Azimuth angle (right). Black line is the trend; red line is the root mean square ..	24
➤ Figure 18: Nyborg station (left), Zenith Tropospheric Delay (right)	25
➤ Figure 19: Zenith Hydrostatic Delay plot (left) and its corresponding Zenith Wet Delay plot (right).....	25
➤ Figure 20: Nyborg station Residual plot as an angle of Elevation angle (left) and as an angle of Azimuth angle (right). Black line is the trend; red line is the root mean square ..	26
➤ Figure 21: Övertorneå station (left), Zenith Tropospheric Delay (right).....	27
➤ Figure 22: Zenith Hydrostatic Delay plot (left) and its corresponding Zenith Wet Delay plot (right).....	27
➤ Figure 23: Övertorneå station Residual plot as an angle of Elevation angle (left) and as an angle of Azimuth angle (right). Black line is the trend; red line is the root mean square ..	28
➤ Figure 24: Oxelösund station (left), Zenith Tropospheric Delay (right)	29
➤ Figure 25: Zenith Hydrostatic Delay plot (left) and its corresponding Zenith Wet Delay plot (right).....	29

- Figure 26: Oxelösund station Residual plot as an angle of Elevation angle (left) and as an angle of Azimuth angle (right). Black line is the trend; red line is the root mean square .. 30
- Figure 27: Stavsnäs station (left), Zenith Tropospheric Delay (right) 31
- Figure 28: Zenith Hydrostatic Delay plot (left) and its corresponding Zenith Wet Delay plot (right)..... 31
- Figure 29: Stavsnäs station Residual plot as an angle of Elevation angle (left) and as an angle of Azimuth angle (right). Black line is the trend; red line is the root mean square .. 32
- Figure 30: Västerås station (left), Zenith Tropospheric Delay (right) 33
- Figure 31: Zenith Hydrostatic Delay plot (left) and its corresponding Zenith Wet Delay plot (right)..... 33
- Figure 32: Västerås station Residual plot as an angle of Elevation angle (left) and as an angle of Azimuth angle (right). Black line is the trend; red line is the root mean square .. 34
- Figure 33: Vindeln station (left), Zenith Tropospheric Delay (right) 35
- Figure 34: Zenith Hydrostatic Delay plot (left) and its corresponding Zenith Wet Delay plot (right)..... 35
- Figure 35: Vindeln station Residual plot as an angle of Elevation angle (left) and as an angle of Azimuth angle (right). Black line is the trend; red line is the root mean square .. 36
- Figure 36: Älvsbyn station comparison plot with ECMWF (left), Comparison with RCA (right). Red line is the overall trend 38
- Figure 37: Gryt station comparison plot with ECMWF (left), Comparison with RCA (right). Red line is the overall trend 38
- Figure 38: Hisingsbacka station comparison plot with ECMWF (left), Comparison with RCA (right). Red line is the overall trend 39
- Figure 39: Nyborg station comparison plot with ECMWF (left), Comparison with RCA (right). Red line is the overall trend 39
- Figure 40: Övertorneå stations comparison plot with ECMWF (left), Comparison with RCA (right). Red line is the overall trend 40
- Figure 41: Oxelösund station comparison plot with ECMWF (left), Comparison with RCA (right). Red line is the overall trend 40
- Figure 42: Stavsnäs station comparison plot with ECMWF (left), Comparison with RCA (right). Red line is the overall trend 41
- Figure 43: Västerås station comparison plot with ECMWF (left), Comparison with RCA (right). Red line is the overall trend 42
- Figure 44: Vindeln station comparison plot with ECMWF (left), Comparison with RCA (right). Red line is the overall trend 42
- Figure 45: Ionospheric delay error sources..... 44
- Figure 46: Good and Bad DOP due to Satellite Geometry 46
- Figure 47: Space weather errors due to the solar activity and ejection of solar flares..... 47
- Figure 48: Choke Ring Antenna (Image courtesy Trimble) 48

List of Tables

- ▶ Table 1: Comparison of the currently four main GNSS systems (Updated: Dec 2011) 7
- ▶ Table 2: Chosen SWEPOS GNSS-Stations with site location and details..... 14
- ▶ Table 3: Shows the RMS of every station, Mean difference of GIPSY computed solution with two climate models and the standard deviation of difference of the GIPSY computed solution with the two independent climate models..... 50

1 Introduction

Today the concept of climate change and global warming has received widespread attention not only from scientists but also from public media and people in general. New media report alarming stories of climate disasters and business companies strive hard to earn climate credibility. In the science community, the notion of climate change is not new. In fact the effects are global is evident from observation of glacier withdrawal and decrease in snow cover in both hemisphere. The scientific question today is not whether there will be a climate change, rather, how severe will this change be, what will actually change and how well can we predict the change.

The important steps in the advancement of atmospheric science were the introduction of observation from different platforms e.g. satellites, space borne aircrafts, radiosondes, balloons etc. Measurement data of the remotest part of earth's atmosphere are now at arm's length and the atmospheric processes and their implications for climate system can be studied on a global scale. Together with ground based observations, these observations are used in global climate models, based on the physical principles that describe the atmospheric and oceanic processes to model past, present and future climate predictions.

GNSS are also routinely been used in weather forecasting, atmospheric research and space weather applications. These days GNSS observations are very likely to become even more important and well suited particularly for climate monitoring and research, as they provide continuous observations of high precision and vertical resolution data under all types of weather conditions and covers the whole earth, apart from its applications in surveying and space geodesy which now become an excellent tool for studying earth atmosphere. The ground based GNSS reference stations shows potential for atmospheric data assimilation and numerical weather predictions. The main advantage of using such technique is it is based on the existing network providing high temporal and special resolution with very low cost and available 24 by 7. Also in the past few years, there has been drastically increase in the use of ground based geodetic receivers to provide data for weather prediction and research in global climate change.

Atmospheric applications of space geodesy are generally increasing scientific interest. Dense GNSS reference stations in Scandinavia, North America, Japan and Europe are now routinely providing data for daily weather forecasts. More interesting but having equally great potential is the detection of GNSS signal reflections from surface primarily oceans and ice. With the prospects of substantially increased signal strength, redundancy and availability in the next decade from GPS, Galileo and other GNSS systems, it may soon become a reality and a next big thing from the space as well.

An interesting fact about the earth's atmosphere is it contains various green house gas constituents. Refractive index of an electromagnetic wave travelling into the atmosphere is also changes due to the presence of these various constituents and this change is responsible for ray

bending and propagation delay of the signal which causes problems in the GNSS based techniques and for the precise observations.

1.1 Structure of the Atmosphere

The atmosphere divided vertically into four layers based on the temperature changes known as Troposphere, Stratosphere, Mesosphere and Ionosphere which is further divided into sub layers, as shown in Figure 1. Gravity pushes the layers down towards earth's surface so the lower layers have more air pressure. All the earth's weather related activity occurs in Troposphere due to the high percentage of water vapor and also including several other atmospheric constituents. The water vapor content decreased significantly above the troposphere and the air becomes drier in the stratosphere and the upper regions.

The Water is an essential part of earth's system and oceans cover nearly three-quarters of the earth surface which plays an important role in exchanging of heat and moisture in the atmosphere. Most of the water vapor in the atmosphere comes from ocean due to the extensive interaction of ocean and atmosphere. Ocean not only acts as an abundant moisture source but also major heat source for the atmosphere.

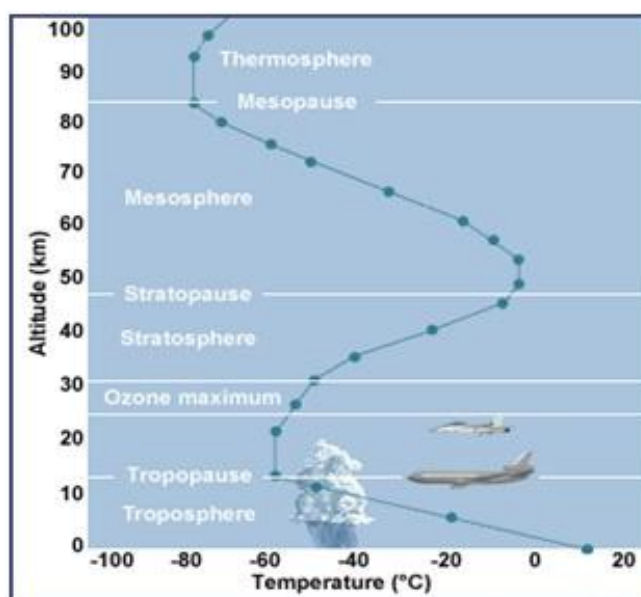


Figure 1: Atmospheric Layers based on Temperature with respect to Altitude¹

Earth's water is always in movement and the earth water cycle describes the continuous movement of water above the surface of the earth. Although the balance of water on the earth remain constant over time and individual water molecules in the form of gas can come and go in a hurry. And since Earth water cycle in truly a water cycle which never stops. During the water cycle, water changes its states from ice to liquid to gas at various places in the water cycle. Also during the water cycle, water is continuously evaporating and condensing in the sky and then precipitation occurs in the form of rain, snow, hail or sleet, shown in Figure 2. But most precipitation falls on earth as rain.

¹ http://www.ucar.edu/learn/1_1_1.htm

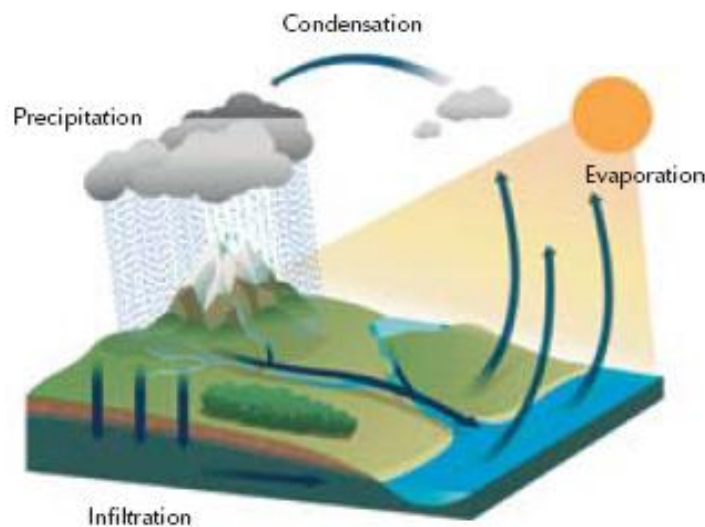


Figure 2: Earth Water Cycle causes a big shift in the Troposphere region includes evaporation, condensation, precipitation and infiltration²

1.2 Motivation

The changes in the earth atmospheric process cause a huge difference in the GNSS data for climate research to predict better changes for the future and in the past decade, the importance of measuring atmospheric constituents has significantly increased. An important fact is the green house gas in the earth's atmosphere contains various constituents including water vapor but due to the presence of GNSS techniques, it is now possible to address all of those constituents which cause the change in refractive index of an electromagnetic wave travelling into the atmosphere which is responsible for the ray bending and propagation delay in the GNSS signal and observations.

The speed of electromagnetic wave is largely affected by some other parameter like temperature, pressure and humidity (water content in the atmosphere) and since these parameters vary in time and space, the Tropospheric delay is also a variable of time and space. Tropospheric delay is a considerable value especially when electromagnetic waves travel through the atmosphere at a low elevation angle.

Tropospheric delay is usually divided into two parts, wet delay (due to water vapor) and the dry delay (due to dry atmosphere). Zenith wet delay (ZWD) is related to the total amount of water vapor along the zenith direction and zenith dry delay or zenith hydrostatic delay (ZHD) is the total amount of dry air along the zenith direction. The sum of these two entities is called the Zenith Tropospheric Delay (ZTD).

The water vapor content estimated from GPS or other GNSS can be useful both in meteorology and climatology. A long time-series of water vapor from GNSS stations could be used to detect trends in the atmospheric water vapor contents, although presently most GPS stations have not been operational but in future these stations would definitely make a huge difference to understand atmospheric water vapor and weather prediction.

² http://water.nationalacademies.org/basics_figures.shtml

The information on the vertical distribution of water vapor is today mainly from radiosonde which are launched only few times per year but in Sweden there are only few number of radiosonde launch sites that are operational. Therefore the study of atmospheric measurement and research especially atmospheric sounding including atmospheric estimated from GNSS data, monitoring climate, forecasting and numerical weather predictions is of huge interest. It is also very important to know the distribution of atmospheric constituents in the atmosphere when making weather forecasts.

1.3 Thesis Structure

In chapter 2, we discuss about the global navigation satellite system and their techniques. We also discuss the latest and upcoming different GNSS systems in the world, their comparison and the details of each system.

In chapter 3, we discuss about the GNSS reference station and their governing bodies in Sweden and all over the world. In the end we also discuss about the different types of reference stations that exist these days.

In chapter 4, we discuss about the selection of data and their processing. We will also discuss about the stations that we selected for this thesis. Later we discuss about the software that we used during this thesis and how it works.

In chapter 5, we will discuss about the method for the processing of data in this thesis and also show you the equations that are used during this thesis.

In chapter 6, we will show you the results of this thesis for the selected GNSS stations in the form of different plots of every station. We will also discuss about the final outcome of the results that we get.

In chapter 7, we compare our final results with other models of independent data sets for the validation part of our thesis

In chapter 8, we talk about different types of error sources that decreases the accuracy of our data of GNSS stations

In chapter 9, we discuss about the final conclusions that we get after finishing this thesis. We will also discuss about the RMS, mean differences and standard deviation of differences

In chapter 10, we will discuss come future work and recommendations because the decisions we make in the future definitely increase the accuracy in GNSS observations

2 GNSS – Global Navigation Satellite System Techniques

Global Navigation Satellite Systems - GNSS are the constellations of satellites designed to provide positioning and timing information for users on Earth and Space. Currently the most widely used operational GNSS is United State's NAVSTAR GPS – Global Positioning System. In addition to GPS, another GNSS that was fully operational in the recent past was the Russian Federation's GLONASS – Global Orbiting Navigation Satellite System.

Despite the popularity of GPS, many users are interested in alternative systems. This is motivated, part, by the fact that GPS is a system operated and controlled by the U.S. Department of Defense. As such, some users may want to retain a navigation capability that is not solely GPS-based. Another more technical motivation for this is due to the fact that GPS (or other GNSS) is a single system, and it is conceivable that a single failure can result is a denial of service to a large number of users. Multiple GNSS may provide a level of redundancy and thus an add degree of robustness to GNSS applications. In addition to GPS and GLONASS, there are other GNSS currently in development, such as European Union's GALILEO – European Global Satellite Navigation Systems, China's COMPASS/BeiDou System.

While GNSS provides an unprecedented level of accuracy and ubiquity of navigation, it has well-known shortcomings. Many of these disadvantages can be significantly curtailed by using integrated navigation systems. For example one such shortcoming is the signal's susceptibility to the unintentional or malicious radio frequency interference or jamming and the fact that the signal cannot provide an attitude or orientation solution easily – a feature that is indispensable in many vehicle navigation and guidance applications. Even though the use of GPS is attitude determination has been demonstrated with considerable success, it requires specialize receivers and multiple antenna separated by some distance. Both the above noted drawbacks can be mitigated by the use of multisensor or integrated navigation systems.

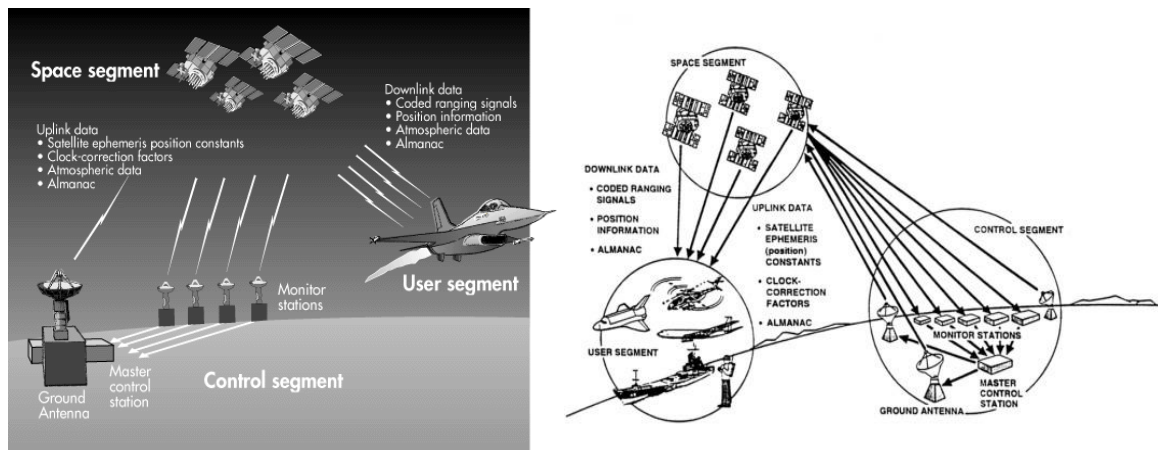


Figure 3: GNSS Segments, Space segment, Control Segment and User Segment³

A Global Navigation Satellite System consists of only three segments: Space segment mainly consists of atomic clocks, transmitters, solar panels and the constellations of satellites. Control segment contains ground stations which continuously monitor every satellite details like maintaining the orbits of the satellites, estimating and uploading the orbit (navigation) information. The last one is the User segment where user have access to it through different applications, see Figure 3. To use GNSS system, one must have a receiver and an antenna.

Satellite navigation is primarily designed for outdoor applications with line of sight visibility to the satellites. However there is an increasing demand for a navigation device that functions reliably indoors. A representative but non-exhaustive list of such applications includes: placing satellite receivers in oceans buoys to measure wave height and direction, monitoring the Earth's crustal deformations, sensing the atmosphere using occultation techniques, location based service – refers to the use of positioning information to enable the additional features on existing devices such as mobile phones, PDAs, tablets etc. Other areas of GNSS applications are aviation, marine, space, automotive, agriculture, forest, geodesy, surveying, scientific application and so on and so forth.

³ <http://www.aero.org/education/primers/gps/elements.html>
http://www.nap.edu/openbook.php?record_id=9254&page=6

	GPS	GLONASS	Galileo	COMPASS
Affiliation	United States	Russia	Europe	China
Satellites	32	23 (30 with CDMA)	2 + 22 (Budgeted)	10 + 30 (Planned)
Orbital Planes	6	3	3	3
Orbital Height (km)	20200	19100	23222	21150
Orbital Period	11 hr 28 min	11 hr 15 min	14 hr 7 min	12 hr 50 min
Orbital Inclination	55	64.8	58	55.5
Multiple Access	CDMA	FDMA/CDMA	CDMA	CDMA
Carrier Frequency (MHz)	<u>1575.42 (L1)</u> <u>1227.60 (L2)</u> 1381.05 (L3) 1379.91 (L4) 1176.45 (L5)	1598.06 – 1605.38 1242.94 – 1248.63	1164 – 1215 1215 – 1300 1559 – 1592	1561.098 1589.742 1268.520 1207.140
Current Status	Fully Operational	Fully Operational (CDMA in preparation)	Partly Operational	Partly Operational

Table 1: Comparison of the currently four main GNSS systems (Updated: Dec 2011)

2.1 GPS:

Global Positioning Systems is the US Military system consist of more the 32 Satellites in six different orbits with approximately 12-hours orbit. The system was designed by US Government but now mostly been used is several civilian applications like space geodesy, atmospheric sounding, weather monitoring and research, guidance and positioning etc, and since being commissioned, it has expanded in the ways that few would have predicted. It is the first and the oldest GNSS system been used all over the world. Table 1 shows more technical details about the system. The highlighted L1 and L2 carrier frequencies have been used during this thesis work. In addition to the scientific applications, a large suite of commercial and public sector users and applications have appeared.

2.1.1 GPS contribution to understand climate change:

To provide instant exact global positioning information, this global positioning system is GPS. Automating and guiding equipment, provide instantaneous services, simplifying total and control survey, for mobile applications that require high accuracy such as 3D-machine control. At least minimum of four satellites must be required and distributed across the sky to receive signal at one point on earth (see DOP – Dilution of Precision). Simply the more satellites you receive the better your system would perform.

2.2 GLONASS:

Today a new positioning satellite constellation in operation called the GLONASS system. This positioning system is maintained and operated by Russian Government much like the GPS in maintained and operated by United States Government. Combining these two satellite constellation will give you access to more than 50-satellites. The additional satellite means stronger and more accurate positions and better performance in obstructed areas in all locations and in all conditions. In 2011, Swedish SWEPOS become the first permanent National GNSS network/infrastructure to use this system due to its higher accuracy at higher latitudes.

2.3 GALILEO:

This GNSS is being designed and implemented by European countries. Galileo is a combination of 30 satellites which can provide global coverage. One of the advantages of European Galileo system is that it's a civilian control global positioning system, unlike the GPS system which is under government control. This guaranteeing continuity of signal and access quality. Unlike GPS and GLONASS, the GALILEO system is initially designed to be a GNSS civilian system that allows access to all users and supply the users with integrity information for the purpose i.e. proving the user with necessary information if the position solution shall not be used for navigation.

When all three systems GPS, GLONASS and GALILEO and fully deployed there would be over 80 satellites, each transmitting several distinct signals providing higher user data, redundancy and more better accuracy.

2.4 COMPASS:

COMPASS GNSS system also known as Beidou2 or BD2 is also one of the GNSS systems designed and implemented by Chinese Government. COMPASS GNSS system consists of more than 30

satellite constellations including GEO and MEO orbit satellites. This system covers entire China and its neighboring Asian countries. It is mostly designed to give coverage for China and East Asian countries.

2.5 Frequency Information

Besides redundancy and increased resistance to jamming, a critical benefit of having two frequencies transmitted from one satellite is the ability to measure directly, and therefore remove the ionospheric delay. In this thesis, we use only L1 and L2 GPS observations to process the data and also to evaluate that how the GNSS system behaves for different geodetic reference stations.

2.6 GNSS Applications

Today, there are several applications have been used and totally rely on the GNSS system in different fields. Like navigations, communications, remote sensing, space geodesy, meteorology/weather and space weather monitoring and other satellite missions like astronomy, cosmology.

There are also number of applications of space geodesy or geodetic data applications like surveying and mappings for civil and construction work, monitoring earthquakes and major other catastrophic disasters by it through continuously monitoring tectonic plate motions. Sea-level measurement by measuring the reflected signals of the sea surface. Machine guidance for demolition, digging, trenches, holes, material handling, lifting, mining etc. In Precise farming for area monitoring, yield and weed monitoring, planting, spraying and harvesting. And in forestry for wildlife tracking and provide precise location in the jungle and remote areas. This thesis focuses of the space geodesy application of GNSS.

3 Ground Based GNSS Network/GNSS Reference Stations

Satellite provides space based platforms to carry out fundamental research about the world we live in, our near and far space. Prior to the development of satellite based scientific missions, our access to the universe was mainly from ground based observations. Use of satellites for scientific research has removed constraints like attenuation and blocking of radiation by earth's atmosphere, gravitational effects on measurements and difficulty in making in-situ measurements or closed studies imposed by earth-based observations. Moreover satellite based scientific research is global by nature and helps in understanding the various phenomena at a global level.

A ground based GNSS Network is a fundamental positioning infrastructure that is supporting GNSS surveying operations in the most efficient way. This sustainable infrastructure is often called "Geodetic Reference Stations" and is composed of several permanent GNSS receivers and antennas, spread out over a specific country.

During the last decade, a large number of permanent GNSS tracking stations have been operating and is continuously increasing due to many geodetic based applications. Those stations are leading to a fairly dense and homogenous worldwide network distribution, supervised by IGS (International GNSS Service), shown in Figure 4.

3.1 IGS Geodetic Stations

The International GNSS service provides the highest quality GNSS data, products and services in support on the earth sciences and research, terrestrial reference frame, earth rotation and for other number of applications including space geodesy, remote sensing, geodynamics etc.

Permanent tracking stations like the global IGS have become valuable in many scientific applications.

Knowledge of zenith wet delay (ZTD) allows us to obtain very interesting value for climatology and meteorology. Integrated or Perceptible water vapor being important for the energy balance of the atmosphere as it holds share of more than 60% of the green house gases. GNSS can therefore

IGS uses the resources and the permanent GNSS geodetic station's data that are used for generating the precise GNSS products like satellite ephemerides, earth rotation parameters, atmospheric parameters, GNSS tracking station coordinates and velocities, zenith Tropospheric path delay estimates, Ionospheric maps etc. The products are used in earth science researches, multidisciplinary application and education purposes. At present time, IGS includes GPS and GLONASS products which will incorporate future GNSS for other application.

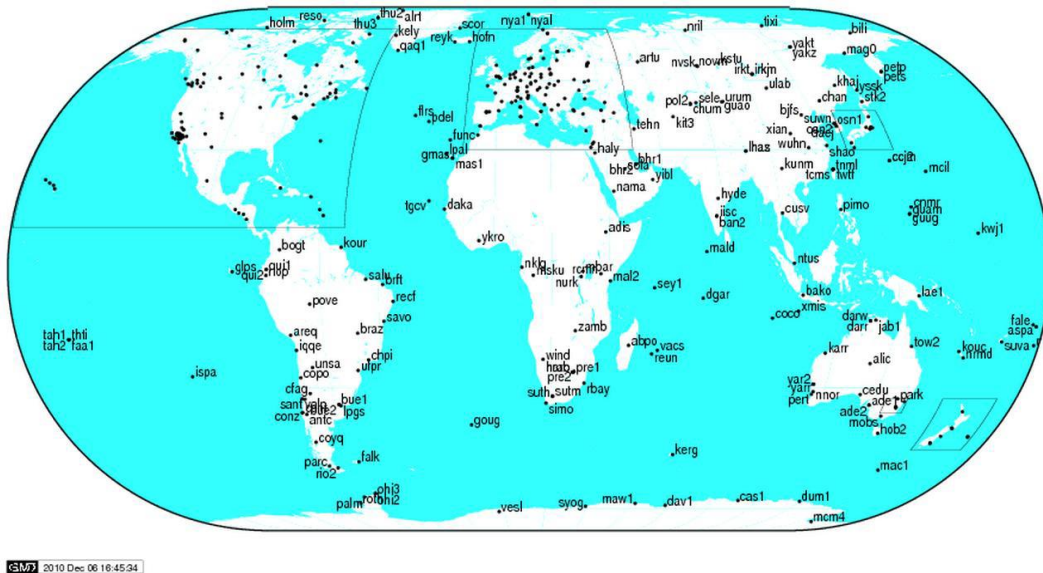


Figure 4: IGS Worldwide Geodetic Stations (image courtesy IGS)⁴

3.2 SWEPOS

SWEPOS - SWEdish Positioning System is a Swedish GNSS based geodetic ground station network that was built up in cooperation between National Land Survey of Sweden (Lantmäteriet), SP Research Institute of Sweden and Chalmers University of Technology Sweden. The first network consists of 5-station and was finished in 1992, today the network is much bigger and consists of more than 200 stations including both first-order and second-order stations, as shown in Figure 5.



Figure 5: SWEPOS GNSS Stations in Sweden, First-order Station (left) Second-order Station (right), (Images courtesy of SWEPOS, Sweden)⁵

⁴ <http://www.igs.org/network/complete.html>

⁵ http://swepos.lmv.lm.se/index_swepos.htm

The first-order stations are the precise permanent stations because they are mounted on stable bedrock where as second-order stations are less precise stations because they are attached on the roof top of a building but not the stable bedrock. Figure 6 shows the distribution of SWEPOS network all over Sweden. The blue circles represent roof top stations and the blue box represents stations of the original stable bedrock. The network is operated by the National Land Survey of Sweden (Lantmäteriet) that is also responsible for the maintenance and future developments.

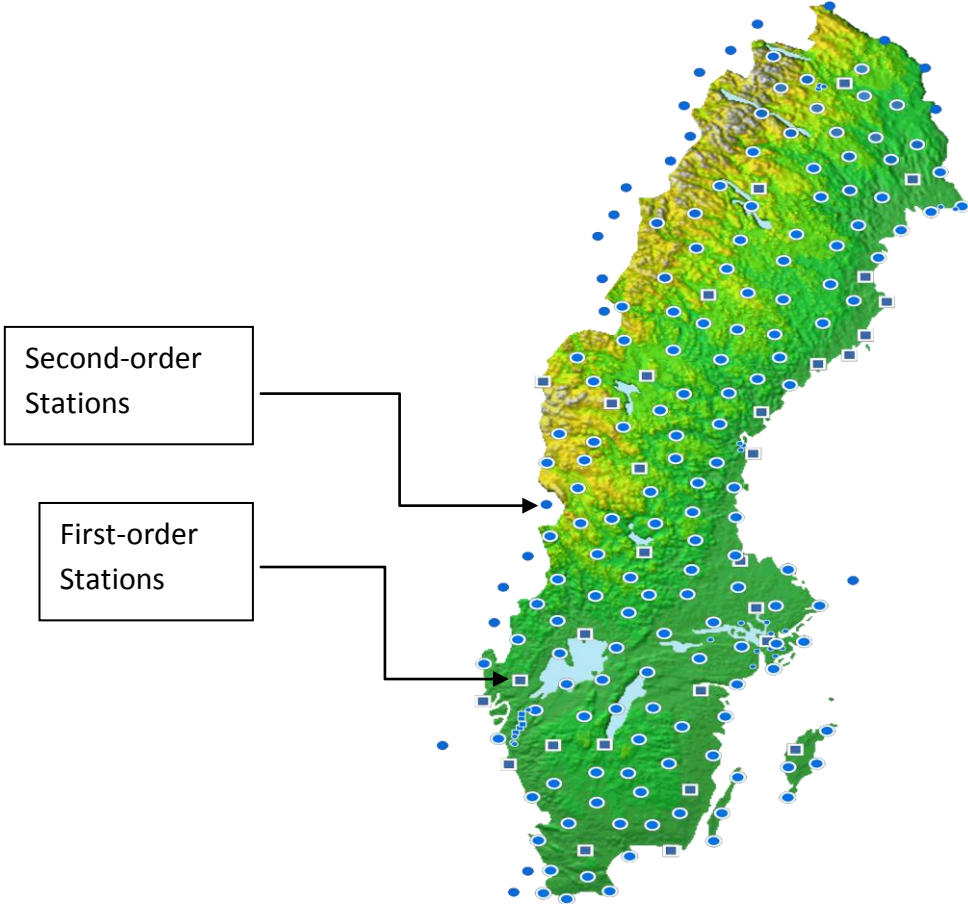


Figure 6: SWEPOS Geodetic Station in Sweden (Image courtesy of SWEPOS Sweden)⁶

For Meteorology and RTK (real time kinematic), worldwide existing stations have been used in order to respond to the continuously increasing requirements in a wide range of applications and scientific studies in geophysics, meteorology and climate because southern hemisphere is mainly covered by oceans and there is still a very lower density of GNSS geodetic tracking sites in this region and in the tropical region.

⁶ http://swepos.lmv.lm.se/pix/sweposkarta_2010-02.gif

4 Data and Processing

Processing of data was done through GIPSY/OASIS software package develop by JPL (Jet Propulsion Laboratory) of NASA (National Aeronautics and Space Administration) of USA. Selections of SWEPOS stations were done randomly from all over Sweden due to the availability of data and to see how the station works in different environment conditions and also to see the stability over longer duration.

4.1 GIPSY/OASIS:

GIPSY-OASIS or simply GIPSY is a GNSS Inferred Positioning System and Orbit Analysis Simulation Software package, developed by CALTECH (California Institute of Technology). GIPSY is not open source software; it requires a license to work. GIPSY is a widely use software for orbit determination. GIPSY does not use double differencing; GIPSY is using PPP (precise-point positioning) for centimeter (cm) level accuracy and it works on the Linux Platform.

The difference between the L1 and L2 phase is used to detect the cycle slips whereas GIPSY uses Melbourne-Wubben Wide Line (MW - WL) to resolve L1 and L2 and then a combination of techniques to determine L1 and L2 cycles separately.

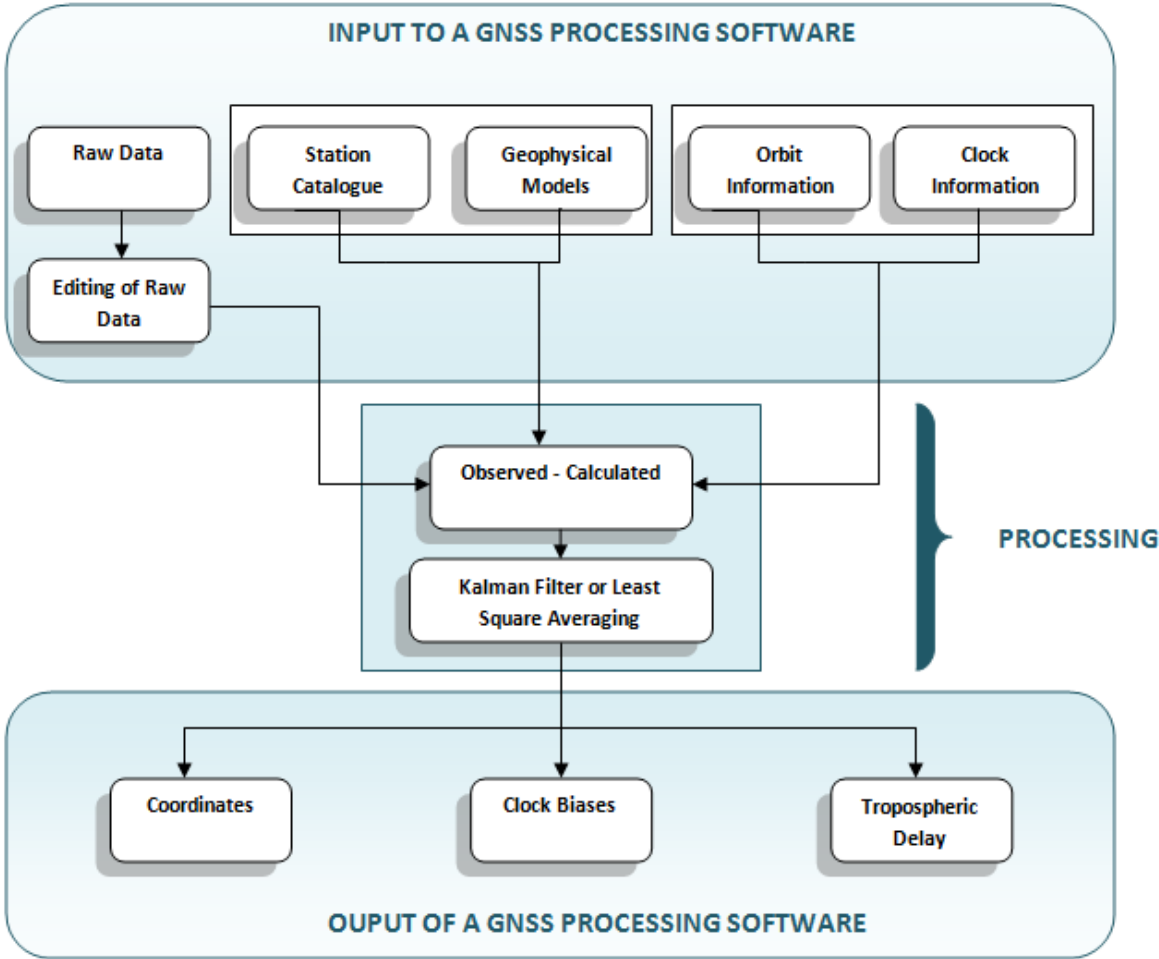


Figure 7: A typical GNSS (GOA-II) software processing

Figure 7 shows the typical processing of GIPSY software where at first the raw data from satellite edited at first then the station catalogue, geophysical models, orbit and clock information are added then the processing is performed by subtracting the calculated values from the observed i.e. O-C is performed. Finally Kalman Filter or Least Square Averaging is performed. Its main purpose is to use measurements observed over time containing noise and other inaccuracies and produce the values that tends to be the closer to the true values. And in the end we get the desired results in the form of coordinated, clock biases and Tropospheric delay measurements.

4.2 Selected Stations and Motivation

The Table 2 shows the randomly selected Nine SWEPOS second-order GNSS stations in Sweden for monitoring Tropospheric Delay, each with their name, station IDs, their locations, station height and the date when each station established,

Station ID	Station Name	Latitude (N) (deg)	Longitude (E) (deg)	Height (meters)	Established Date
ALB0	Älvsbyn	65.67398	21.006935	75.862	2006-06-14
GRY0	Gryt	58.186663	16.800849	53.733	2004-08-20
HIS0	Hisingsbacka	57.732354	11.732354	63.699	2004-10-13
NYB0	Nyborg	66.795913	23.170021	38.416	2006-07-25
OVT0	Övertorneå	66.385718	23.6587	100.582	2006-05-19
OXE0	Oxelösund	58.670953	17.107038	46.758	2002-02-04
STA0	Stavsnäs	59.308861	18.693254	35.902	2001-02-21
VAS0	Västerås	59.64568	16.56136	68.483	1999-03-05
VIN0	Vindeln	64.202226	19.714043	217.959	2006-06-29

Table 2: Chosen SWEPOS GNSS-Stations with site location and details

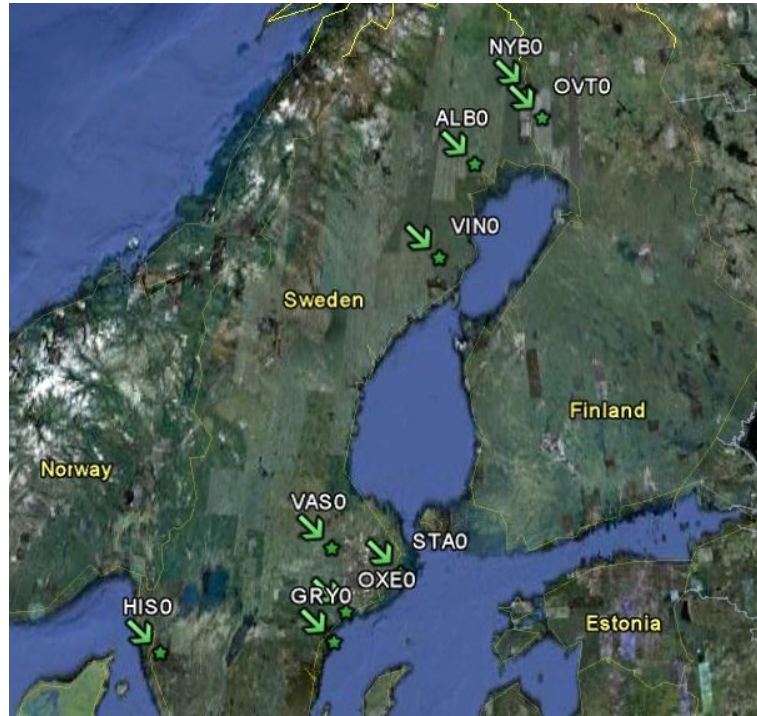


Figure 8: Selected second-order SWEPOS stations, green pointer on the map (Image courtesy google earth)

Selection of SWEPOS stations were done randomly and details are shown in the Table 2. An important thing here to mention is these second-order stations are not very old and are newly build with an average of only 5-years old. Figure 8 shows the geographical locations of every station all over Sweden.

4.3 Data Selection and Motivation

Selection of data for each station was taken place from year 2008 to 2011, all year round includes data for 24-hours of every single day which includes every seasonal and every weather condition like, rain, snow, hailstorm, thunderstorm, fog, dense clouds, sunny, clear sky etc. As this is very short but due to the complexity, handling and processing of data through GIPSY OASIS II, it takes a large amount of time to process for a very short duration of data. But these three years data are more than good enough to analyze each station's performance in every weather condition. Also this short duration gives us some in depth and clear understanding of how everything works, what things are necessary to consider, knowledge about environment and how it impacts our data and in contrast how our system deals with that.

One of the main reasons about the limited amount of data is the availability of data and on top of that is the fact that this data has been updated after every 300 seconds (5-minutes) and if we process a bit more data than it takes a huge amount of time even for the super fast computers to process.

4.4 Chosen Duration and Motivation

The main motive for selecting the duration of my chosen stations are fact that most of the stations are newly build so we don't have data for longer durations and for some stations we have limited duration of data availability. The 03-years data from 2008 to 2011 including all seasonal data updated after every 5-minutes or 300-seconds has been selected to check the stability over the longer durations and to see how each station behaves in different environment scenarios. Another thing here to notice that the trend of Tropospheric delay increases 13% per decade and moisture is correlated with temperature so in future it would definitely be increased or remain same but would definitely not decrease.

5 Method

For processing the raw data from GPS observation, we use statistical/analytical method to collect, organize, analyze and interpret the data. Elevation angle selected here for the processing is 10 degrees due to the fact that it gives the best possible result with very less noise compared to the previously used 15 and 5 degrees. GOA – II (GIPSY/OASIS – II) has been used for processing the raw data of each station which works in Linux Platform using PPP (Precise Point Positioning) strategy which provides the best possible accuracy of up to Centimeter (cm). GOA – II also has tendency to work as real and non-real time capability. In our case we use non-real time GOA – II but for processing the real time data, one must have RTG – Real Time GOA – II. The raw data from GNSS observations are obtained in RINEX (receiver independent exchange) format which are processed using GIPSY software package to obtain the desired output in form of residuals and atmospheric delay plots. If the time series and ground pressure is known then the absolute ZTD is equals to the IPWV (Integrated perceptible water vapor).

5.1 Fundamental Equations

In this section we discuss the few fundamental equations that we use during this thesis to calculate the Tropospheric delay. The ZTD (zenith Tropospheric delay) is generally divided into two separate parts: the ZHD (zenith hydrostatic) and ZWD (zenith wet delay), as shown below,

$$\mathbf{ZTD = ZHD + ZWD}$$

The ZHD is the larger term around 2300 mm at sea levels where as ZHD has the smaller value up to 300 mm. The ZHD can be modeled accurately from the surface atmospheric pressure, height of the station and the latitude. Here the Zenith hydrostatic delay (ZHD) is proportional to the ground pressure and less dependent on the latitude and station height. For ZWD case, it changes temporarily in an unpredictable manner.

$$\mathbf{ZHD = (2.2768.10^{-3} \pm 5.10^{-7}) \frac{P_o}{f(\lambda, H)}}$$

$$\mathbf{f(\lambda, H) = [1 - 2.66.10^{-3} \cos 2\lambda - 2.8.10^{-7}H]}$$

The processing of the GNSS data are regularly performs using standard a priori values for ZHD, independent of the atmospheric conditions over geodetic station. This may be sufficient approximation which can be derived from the topographical model if the ground pressure is not known or available. On the other hand, ZWD is very difficult to model due to the highly variable atmosphere.

This can be unrealistic if only few observations are available or the atmospheric conditions over the geodetic station are unknown or neglected like the pressure. GOA-II uses the station dependent constant a priori value for ZTD. Not using accurate surface pressure leads to the increase in errors in a priori value of ZHD which in turn decrease the accuracy of ZTD values in the analysis. Both ZHD and ZWD have similarities in elevation angle dependence but only one parameter is used to estimate corrections for the combined effect of hydrostatic and wet delay. Also we need some assumptions which are near to the real of that epoch to calculate other parameter. The correction of the a priori is smaller which means the a priori vales are closer to the real values thus a better accuracy can be achieved.

6 Results

6.1 Älvsbyn

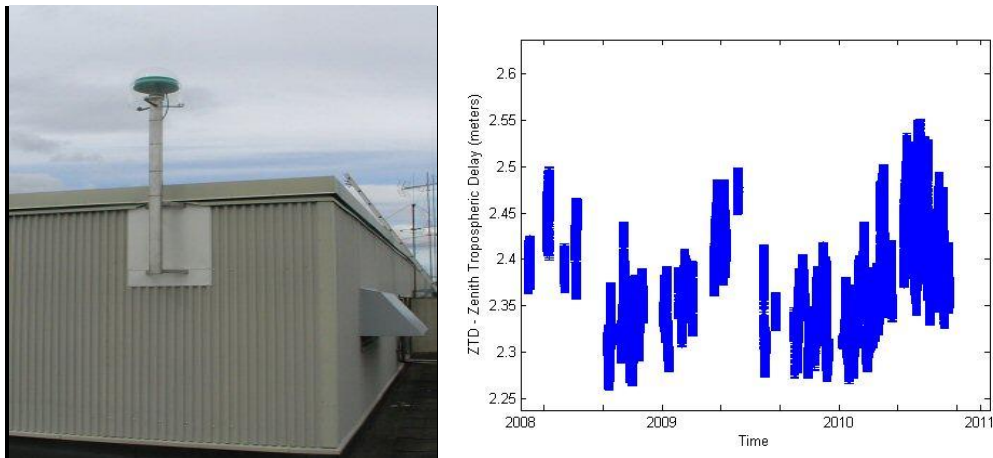


Figure 9: Älvsbyn station (left), Zenith Tropospheric Delay (right)

Älvsbyn station (ALB0) is established in 2006. It is located in the Norrbotten Län (county) in northern Sweden. Figure 9 shows the station ALB0 which is located in the (area type) with LAT 65.674° , LON 21.006° and station height 78.15m (above sea level). Figure 10 shows the ZTD trend of last 3-years. Figure 11 shows the mean residuals in centimeter as a function of elevation and azimuth angles in degrees, each with the estimated root mean square. The residuals plots are very good and in an envelope shape. There are some minor scattering and reflection in some directions but overall it's a very good station with perfect environment.

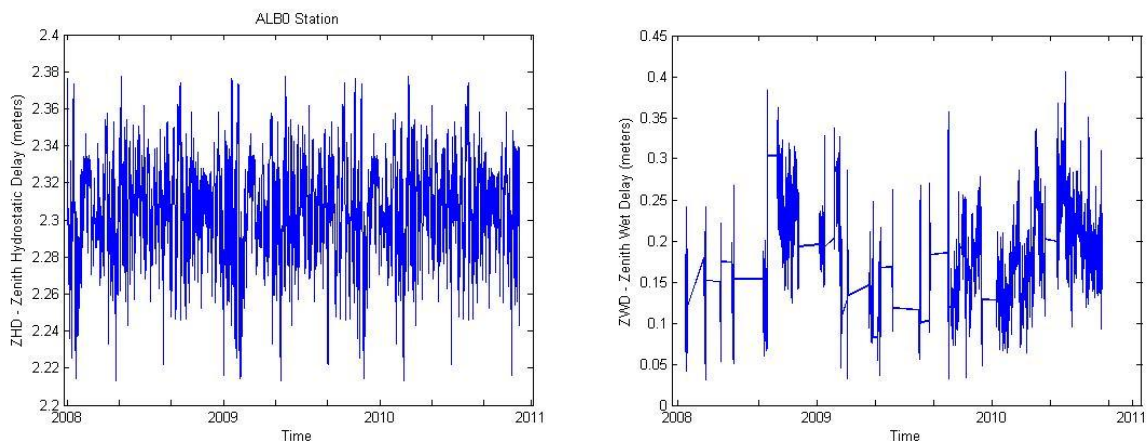


Figure 10: Zenith Hydrostatic Delay plot (left) and its corresponding Zenith Wet Delay plot (right)

Figure 9 and Figure 10 of the ZTD and ZWD plots shows some gaps at different epochs. The gaps in the end after September 2010 are due to the unavailability of the data and the other gaps are due to having some difficulties with the data itself which makes it even hard to process for the GIPSY script. ZTD and ZWD plots are based on the GIPSY software package and cannot be plotted

through models due to the rapid change in the atmosphere. On the other hand, the ZHD plot of Figure 10 show a continuous plot which is based on the model that depends only on the station surface pressure, station height and the latitude.

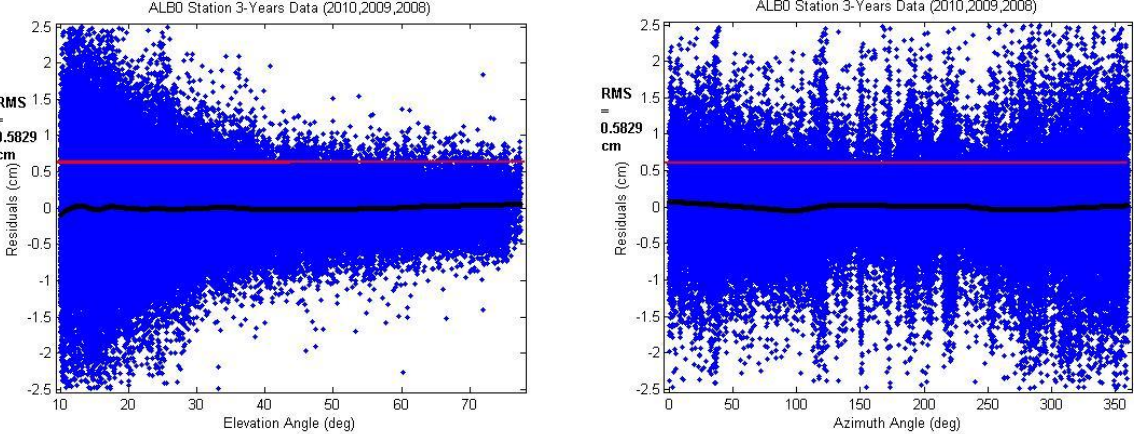


Figure 11: Älvsbyn station Residual plot as an angle of Elevation angle (left) and as an angle of Azimuth angle (right). Black line is the trend; red line is the root mean square

6.2 Gryt

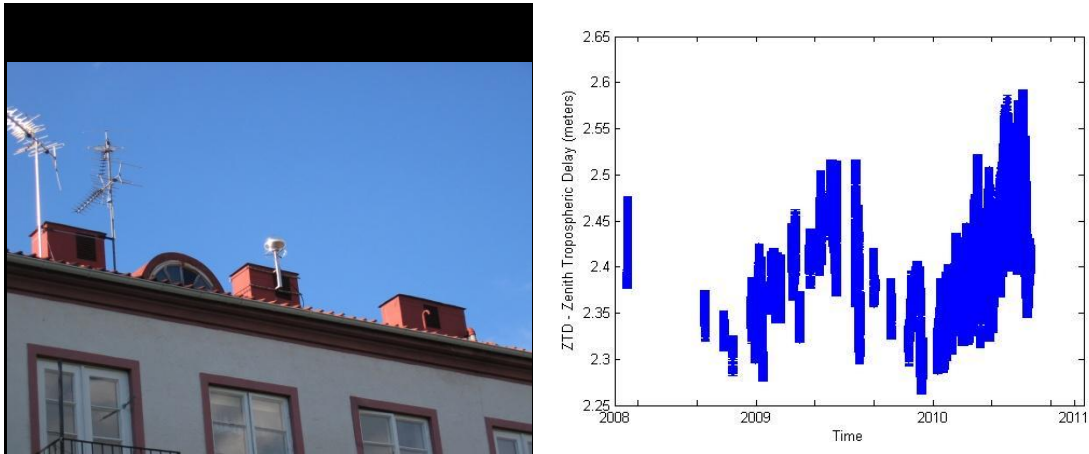


Figure 12: Gryt station (left), Zenith Tropospheric Delay (right)

Gryt Station (GRY0) was established in 2004. It is located in Östergötlands Län with LAT 58.186° , LON 16.00° and height 53.80 meters (above sea level). The station is located above the buildings which are also surrounded by other residential area (see Figure 12). Figure () shows the ZTD trends from year 2008 to 2011. Figure 13 shows the ZHD and ZWD trend for the same years which is very much satisfies the required trend should be. And Figure 14 shows the mean residuals (in cm) of year 2008 to 2011 as a function of elevation and azimuth angles (in degree). The postfit residuals plot shows some disturbances in a particular directions and we can also see there are some other antenna that are close to it are the main reasons for some scattering but overall it's a very good environment for second-order stations.

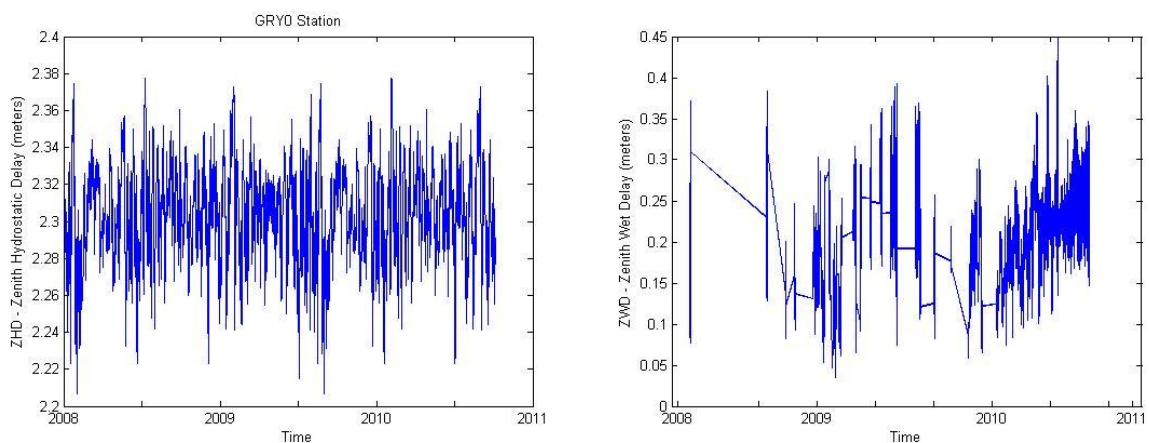


Figure 13: Zenith Hydrostatic Delay plot (left) and its corresponding Zenith Wet Delay plot (right)

Figure 12 and Figure 13 of the ZTD and ZWD plots shows some gaps at different epochs. The gaps in the end after September 2010 are due to the unavailability of the data and the other gaps are

due to having some difficulties with the data itself which makes it even hard to process for the GIPSY script. Some small gaps are also due to the GIPSY processing that we face during this thesis due to the GIPSY script limitations. ZTD and ZWD plots are based on the GIPSY software package and cannot be plotted through models due to the rapid change in the atmosphere. On the other hand, the ZHD plot of Figure 10 show a continuous plot which is based on the model that depends on only station surface pressure, station height and the latitude.

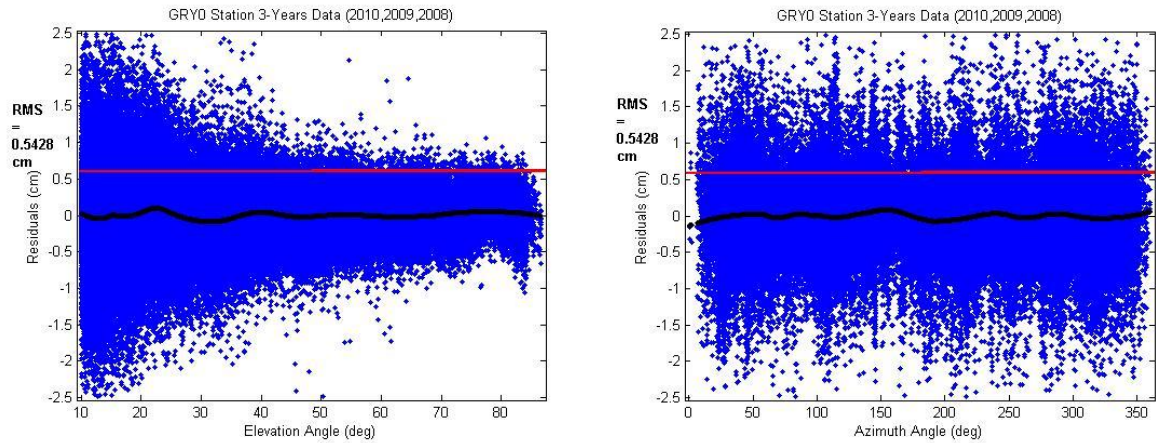


Figure 14: Gryt station Residual plot as an angle of Elevation angle (left) and as an angle of Azimuth angle (right). Black line is the trend; red line is the root mean square

6.3 Hisingsbacka

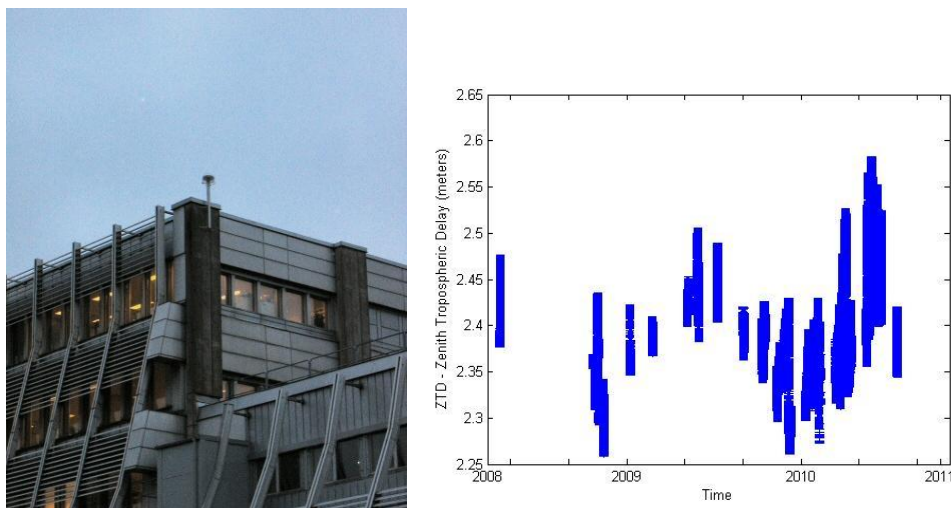


Figure 15: Hisingsbacka station (left), Zenith Tropospheric Delay (right)

Station Hisingsbacka (HISO) is located outside of Gothenburg in Västra Götalands Län (region). HISO station was established in 2004 and built on the roof top of building surrounded by trees and mostly vegetation (see Figure 15). It is situated at LAT 57.732° , LON 11.986° and height 63.734 meters (above ground level). The ZTD trends of year 2008 to year 2011 are also shown in meters. The ZHD and ZWD trends are shown in Figure 16. Finally the means residuals (in cm) are plotted and shows in Figure 17, each with estimated RMS (in cm) with function of elevation and azimuth angles (in degrees).

The postfit residuals plot as azimuth angle shows some multipath reflections and scattering in all directions due to very close object environment.

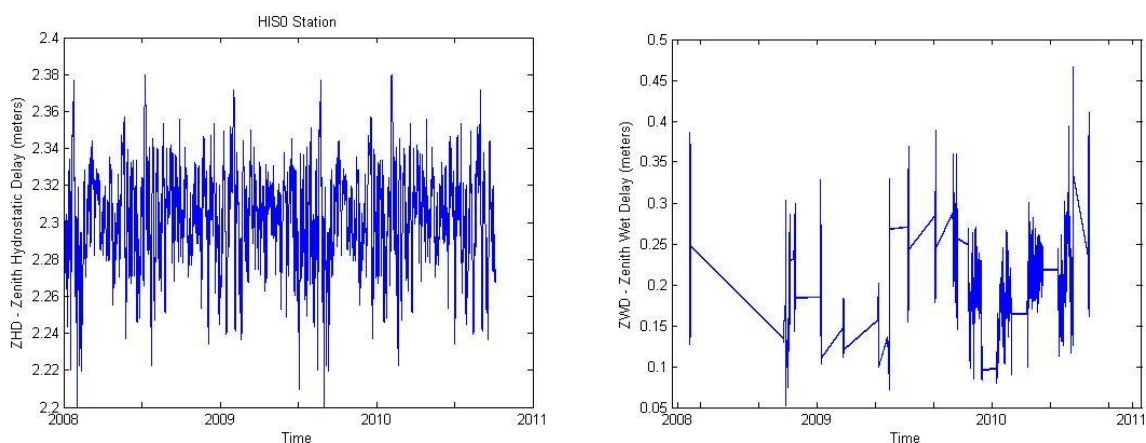


Figure 16: Zenith Hydrostatic Delay plot (left) and its corresponding Zenith Wet Delay plot (right)

Figure 15 and Figure 16 of the ZTD and ZWD plots shows some gaps at different epochs. Some small gaps are also due to the GIPSY processing that we face during this thesis due to the GIPSY script limitations. The gaps in the end after September 2010 are due to the unavailability of the

data and the other gaps are due to having some difficulties with the data itself which makes it even hard to process for the GIPSY script. ZTD and ZWD plots are based on the GIPSY software package and cannot be plotted through models due to the rapid change in the atmosphere. On the other hand, the ZHD plot of Figure 16 show a continuous plot which is based on the model that depends on only station surface pressure, station height and the latitude.

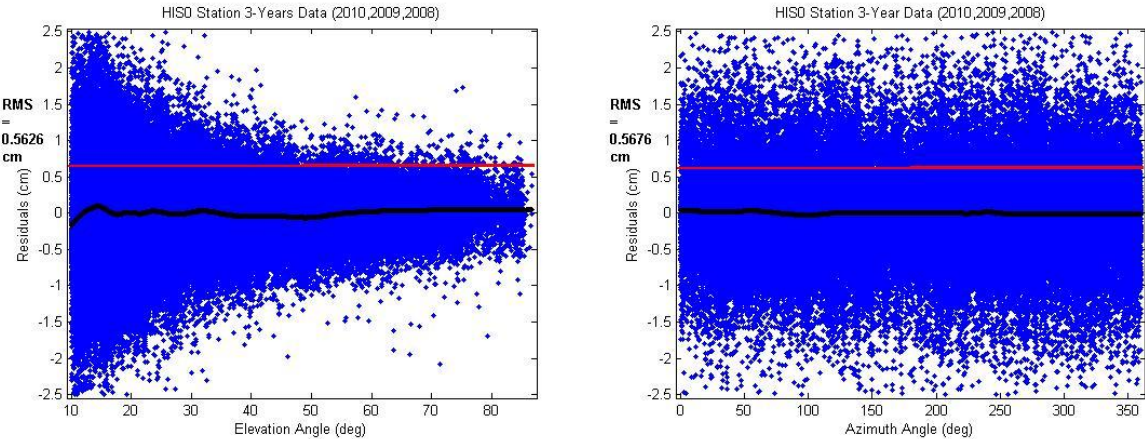


Figure 17: Hisingsbacka station Residual plot as an angle of Elevation angle (left) and as an angle of Azimuth angle (right). Black line is the trend; red line is the root mean square

6.4 Nyborg

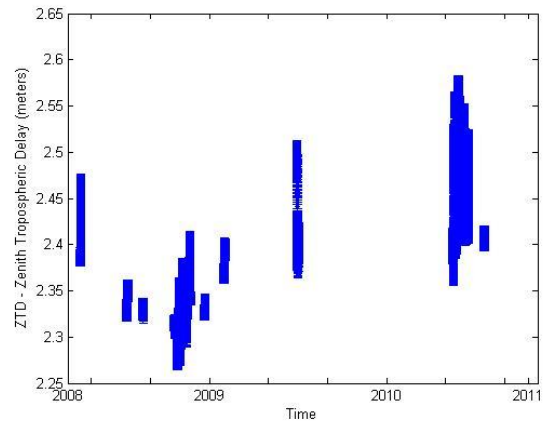


Figure 18: Nyborg station (left), Zenith Tropospheric Delay (right)

The second-order station of SWEPOS Nyborg (NYB0) is located in Norrbottens län, very north of Sweden, established in 2006. NYB0 station coordinates are LAT 65.795° , LAN 23.170° and height 38.523 meters (above ground level). This station is largely surrounded by vegetation. Figure 18 shows the last three years trend in ZTD (in meters) with Figure 19 shows its corresponding ZHD and ZWD trends (also in meters). Mean residuals (in cm) are plotted with respect to both elevation and azimuth angles (in degrees), as shown in Figure 20. The post fit plots for error are very good and in an envelope shape. Some disturbance can be seen in some particular direction as we can see only one side of the station but don't know what's on the other side.

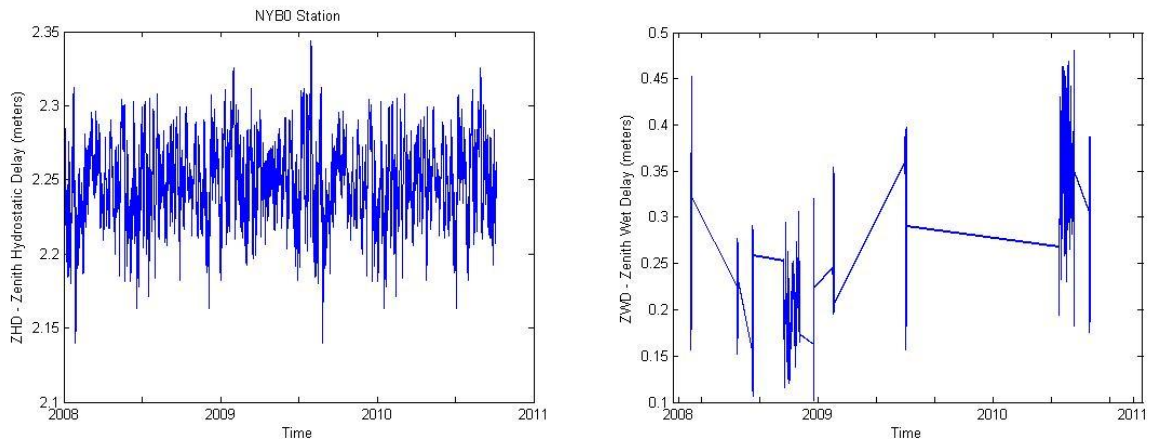


Figure 19: Zenith Hydrostatic Delay plot (left) and its corresponding Zenith Wet Delay plot (right)

Figure 18 and Figure 19 for Nyborg station of the ZTD and ZWD plots shows some gaps at different epochs. The gaps in the end after September 2010 are due to the unavailability of the data and the other gaps are due to having some difficulties with the data itself which makes it even hard to process for the GIPSY script. Some small gaps are also due to the GIPSY processing that we face during this thesis due to the GIPSY script limitations. ZTD and ZWD plots are based

on the GIPSY software package and cannot be plotted through models due to the rapid change in the atmosphere. On the other hand, the ZHD plot of Figure 19 show a continuous plot which is based on the model that depends only on the station surface pressure, station height and the latitude.

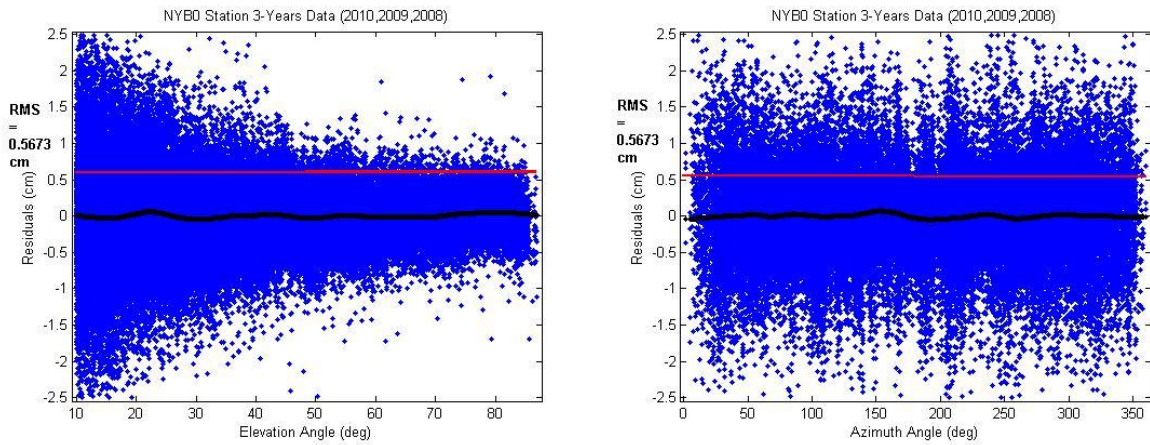


Figure 20: Nyborg station Residual plot as an angle of Elevation angle (left) and as an angle of Azimuth angle (right). Black line is the trend; red line is the root mean square

6.5 Övertorneå

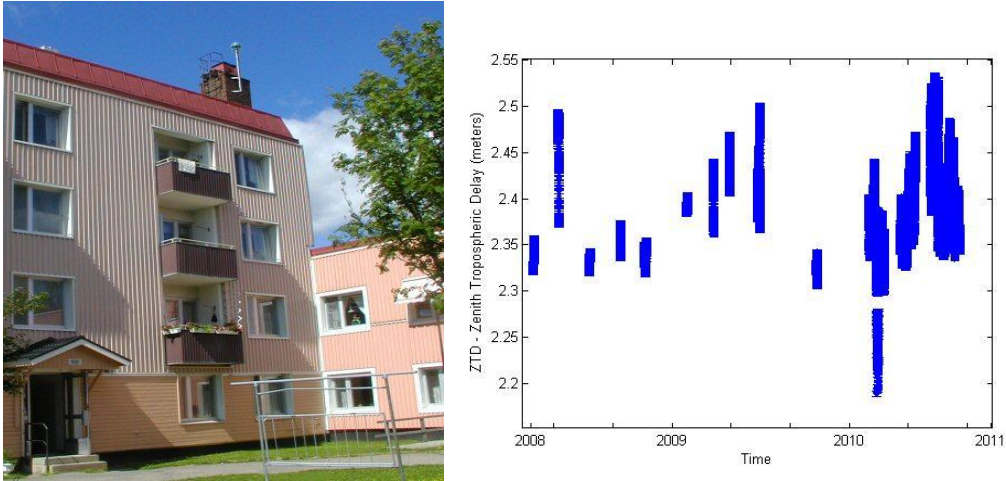


Figure 21: Övertorneå station (left), Zenith Tropospheric Delay (right)

This station of SWEPOS is situated in the populated area of Övertorneå in the Norrbottens Län (region), shown in Figure 21. OVT0 station was established in 2006 in the roof top of building with LAT 66.385° , LON 23.658° and height 100.69 meters (above ground level). The raw data of this GNSS station was processed and finally plotted to see the ZTD trends of last three years in meters. Its respective ZWD and ZHD trends are also shown in Figure 22 of the same duration. At the end the mean residuals are plotted and shown in Figure 23 with function elevation and azimuth angles (both in degrees), each with RMS which is also in centimeters. From the station figure we can assume this station to be very much surrounded by nearby buildings and trees but from the post fit residuals plot it shows the best possible result with only few scattering and reflections in some directions.

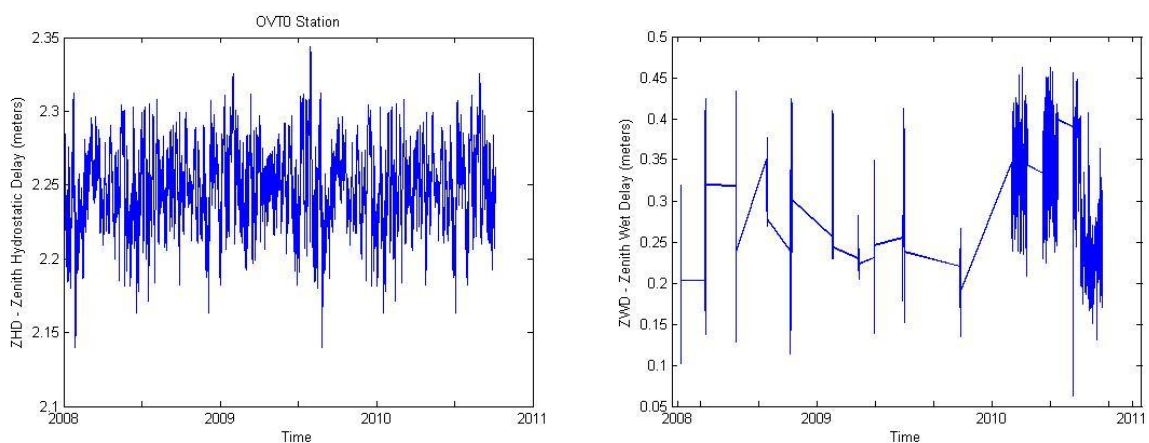


Figure 22: Zenith Hydrostatic Delay plot (left) and its corresponding Zenith Wet Delay plot (right)

Figure 21 and Figure 22 of the ZTD and ZWD plots shows some gaps at different epochs. Some small gaps are also due to the GIPSY processing that we face during this thesis due to the GIPSY

script limitations. The gaps in the end after September 2010 are due to the unavailability of the data and the other gaps are due to having some difficulties with the data itself which makes it even hard to process for the GIPSY script. ZTD and ZWD plots are based on the GIPSY software package and cannot be plotted through models due to the rapid change in the atmosphere. On the other hand, the ZHD plot of Figure 22 show a continuous plot which is based on the model that depends only on station surface pressure, station height and the latitude.

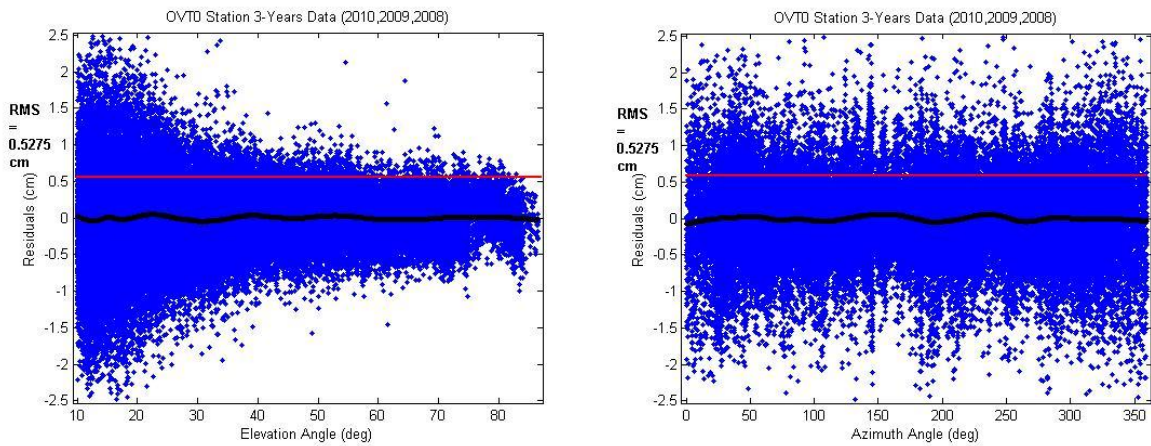


Figure 23: Övertorneå station Residual plot as an angle of Elevation angle (left) and as an angle of Azimuth angle (right). Black line is the trend; red line is the root mean square

6.6 Oxelösund

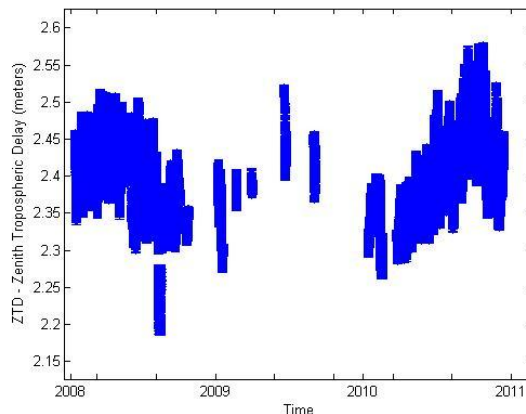


Figure 24: Oxelösund station (left), Zenith Tropospheric Delay (right)

SWEPOS second-order station Oxelösund (OXE0) is one of the oldest station, established in 2002 in Oxelösund city near Nuköping in the Södermanlands Län (region). It is located at LAT 58.670° , LON 17.107° and height 46.84 meters (above ground), see Figure 24. This station is situated in residential area all with surrounded with building and trees. Figure 24 also indicated the zenith Tropospheric delay in meters of last three years in meters. Its corresponding ZHD and ZWD trends are shown in Figure 25. At the end the Figure 26 indicates the mean residuals trend in centimeters with function of both elevation and azimuth angles. We can also see some data points missing which are mainly due to the blockage as this station build below the horizon of the surrounding objects but still it works very good. Finally the root mean square trend was plotted to see the trends in residuals in centimeters.

The red box shows the data that was processed after correcting error in GIPSY script.

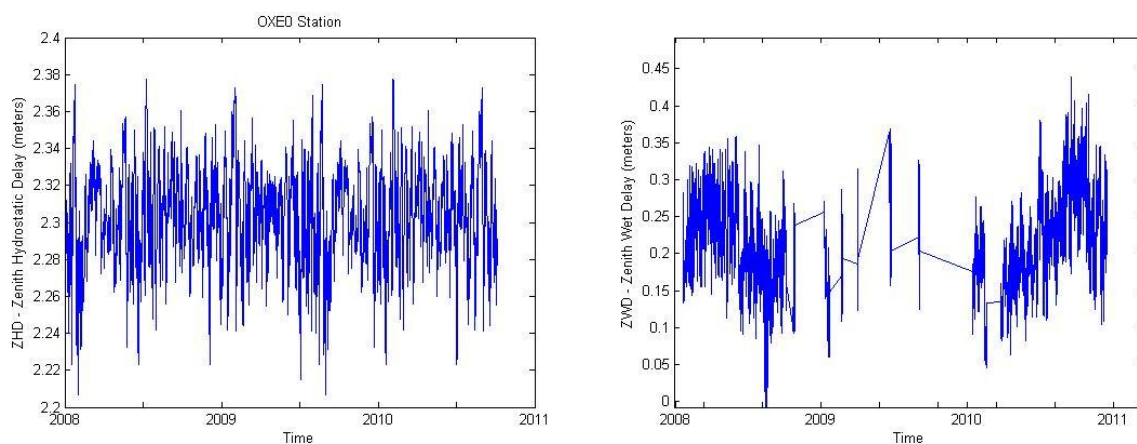


Figure 25: Zenith Hydrostatic Delay plot (left) and its corresponding Zenith Wet Delay plot (right)

Figure 24 and Figure 25 of the ZTD and ZWD plots shows some gaps at different epochs. The gaps in the end after September 2010 are due to the unavailability of the data and the other gaps are

due to having some difficulties with the data itself which makes it even hard to process for the GIPSY script. Some small gaps are also due to the GIPSY processing that we face during this thesis due to the GIPSY script limitations. We also edit the GIPSY script and process the data again for only year 2009 due to the limitation of time and now these ZTD and ZWD plot shows very agreeable results with no gaps in year 2009. ZTD and ZWD plots are based on the GIPSY software package and cannot be plotted through models due to the rapid change in the atmosphere. On the other hand, the ZHD plot of Figure 25 show a continuous plot which is based on the model that depends only on the station surface pressure, station height and the latitude.

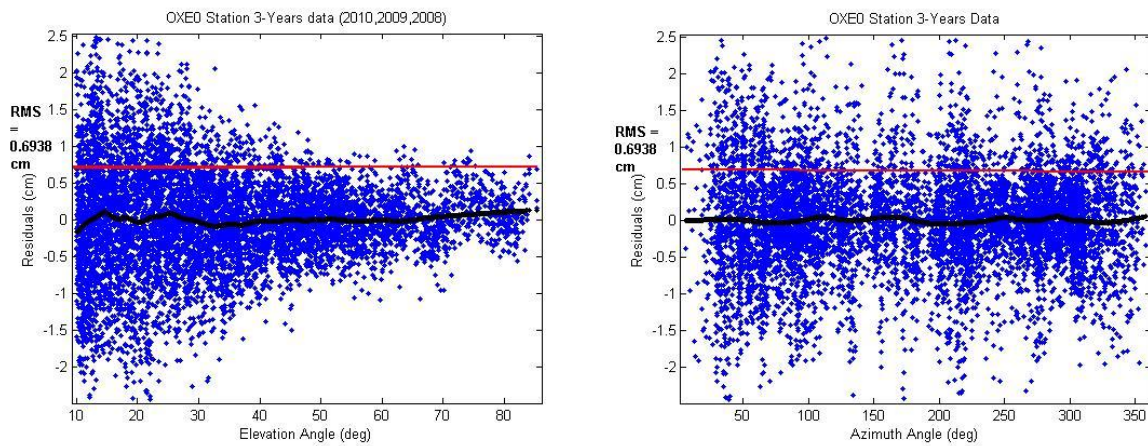


Figure 26: Oxelösund station Residual plot as an angle of Elevation angle (left) and as an angle of Azimuth angle (right). Black line is the trend; red line is the root mean square

6.7 Stavsnäs

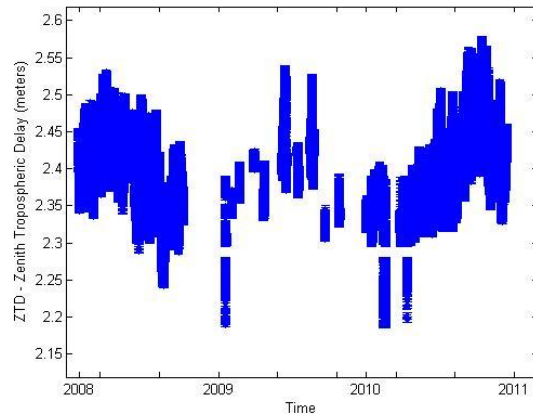


Figure 27: Stavsnäs station (left), Zenith Tropospheric Delay (right)

Station Stavsnäs (STA0) was established east of Stockholm city in 2001 in Värmdö Municipality. This site is located at LAT 59.308°, LON 18.693° and height 35.995 meters above ground. This second-order SWEPOS station is placed on the roof top with largely surrounded by building and trees. Figure 27 shows the Tropospheric delay trend at zenith in meters of the last three years with its respective wet delay and hydrostatic delay both at zenith, shown in Figure 28. Some blockage can be seen in the post fit residuals plot due to the surrounding trees and other reflected objects in Figure 29.

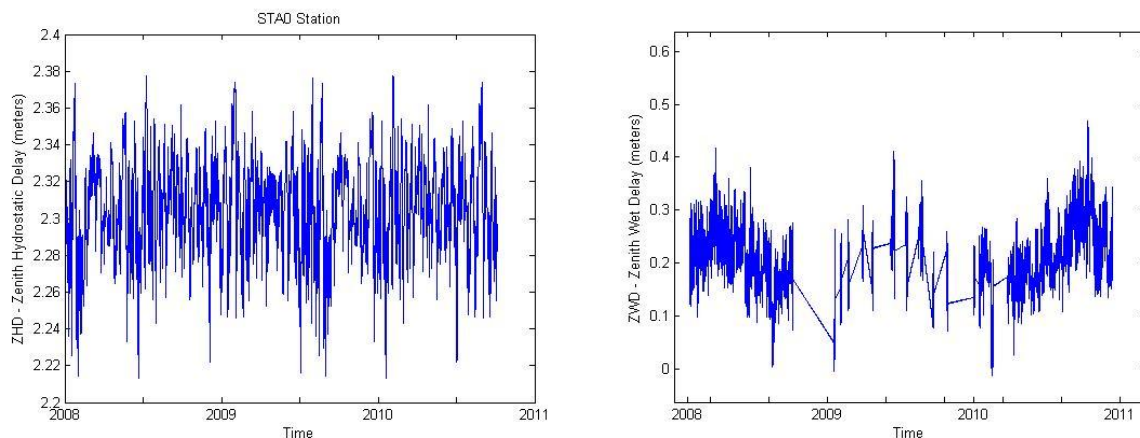


Figure 28: Zenith Hydrostatic Delay plot (left) and its corresponding Zenith Wet Delay plot (right)

Figure 27 and Figure 28 of the ZTD and ZWD plots shows some gaps at different epochs. The gaps in the end after September 2010 are due to the unavailability of the data and the other gaps are due to having some difficulties with the data itself which makes it even hard to process for the GIPSY script. Some small gaps are also due to the GIPSY processing that we face during this thesis due to the GIPSY script limitations. We also edit the GIPSY script and process the data again for only year 2009 due to the limitation of time and now these ZTD and ZWD plot shows very agreeable results with no gaps in year 2009. ZTD and ZWD plots are based on the GIPSY software

package and cannot be plotted through models due to the rapid change in the atmosphere. On the other hand, the ZHD plot of Figure 28 show a continuous plot which is based on the model that depends only on the station surface pressure, station height and the latitude.

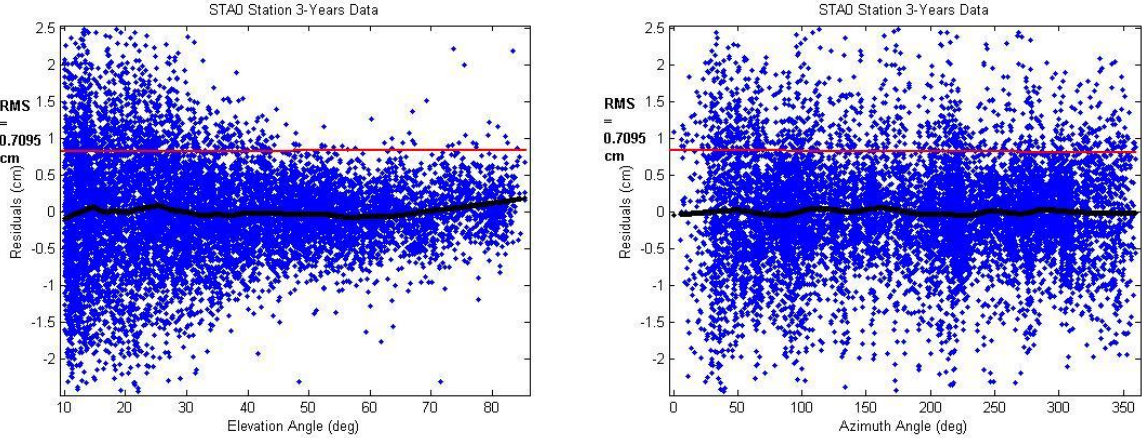


Figure 29: Stavsnäs station Residual plot as an angle of Elevation angle (left) and as an angle of Azimuth angle (right). Black line is the trend; red line is the root mean square

6.8 Västerås

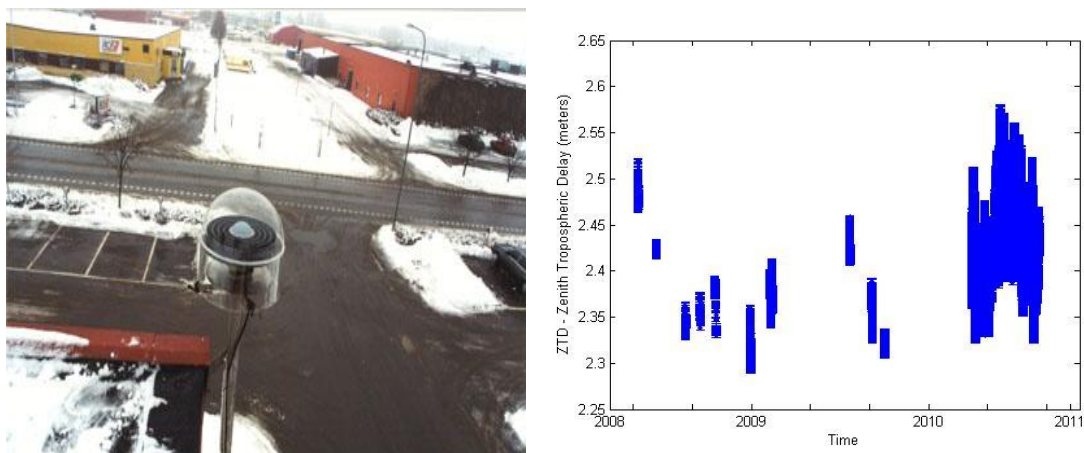


Figure 30: Västerås station (left), Zenith Tropospheric Delay (right)

Figure 30 shows the station Västerås (VASO) situated in city Västerås in Västerås Municipality. Its station coordinates are LAT 59.645° , LON 16.561° and height 68.57 meter above ground. This station is also one of the oldest SWEPOS second-order station, established in 1999. The last three years trend in ZTD (in meters) is shown in the same figure and its corresponding ZHD and ZWD trends (also in meters) in Figure 31. Mean residuals (in cm) are plotted with respect to both elevation and azimuth angles (in degrees) are similar to the other SWEPOS stations with in perfect envelop shape, shown in Figure 32.

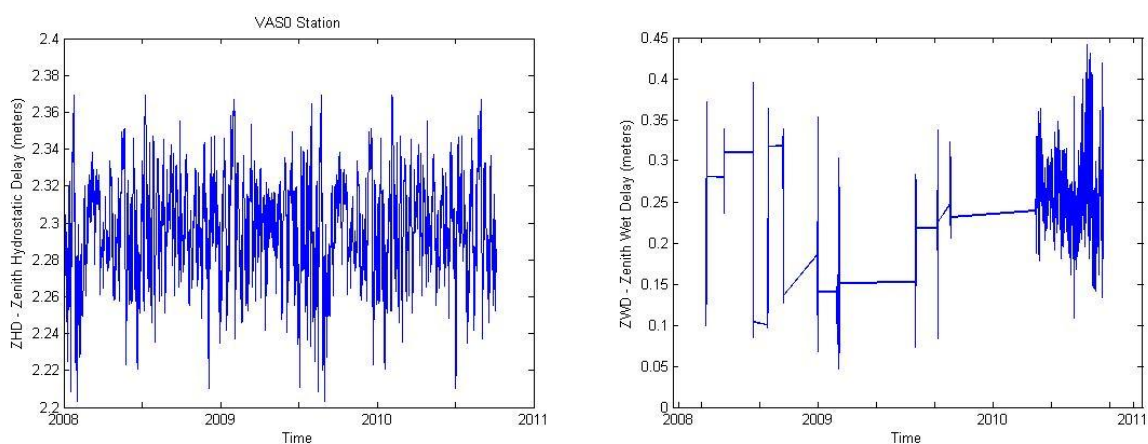


Figure 31: Zenith Hydrostatic Delay plot (left) and its corresponding Zenith Wet Delay plot (right)

Figure 30 and Figure 31 of the ZTD and ZWD plots shows some gaps at different epochs. The gaps in the end after September 2010 are due to the unavailability of the data and the other gaps are due to having some difficulties with the data itself which makes it even hard to process for the GIPSY script. ZTD and ZWD plots are based on the GIPSY software package and cannot be plotted through models due to the rapid change in the atmosphere. On the other hand, the ZHD plot of

Figure 31 show a continuous plot which is based on the model that depends on only station surface pressure, station height and the latitude.

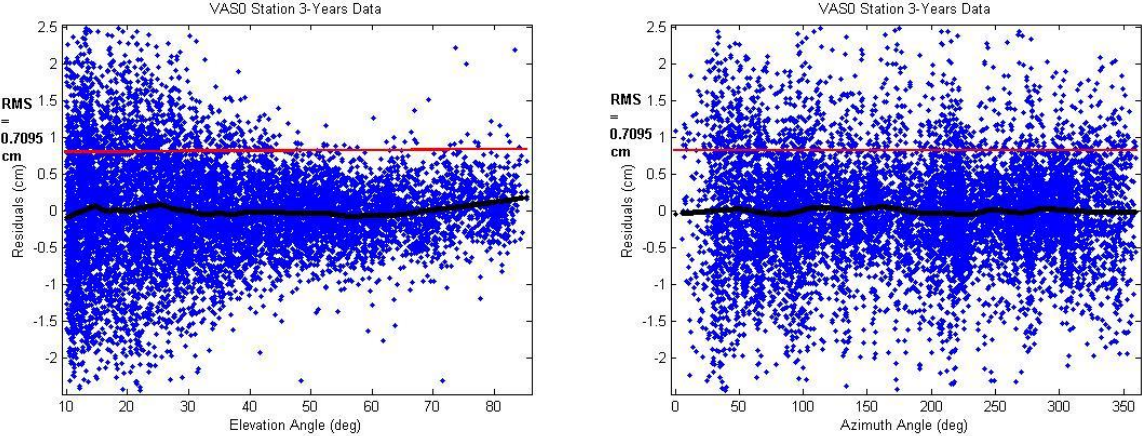


Figure 32: Västerås station Residual plot as an angle of Elevation angle (left) and as an angle of Azimuth angle (right). Black line is the trend; red line is the root mean square

6.9 Vindeln

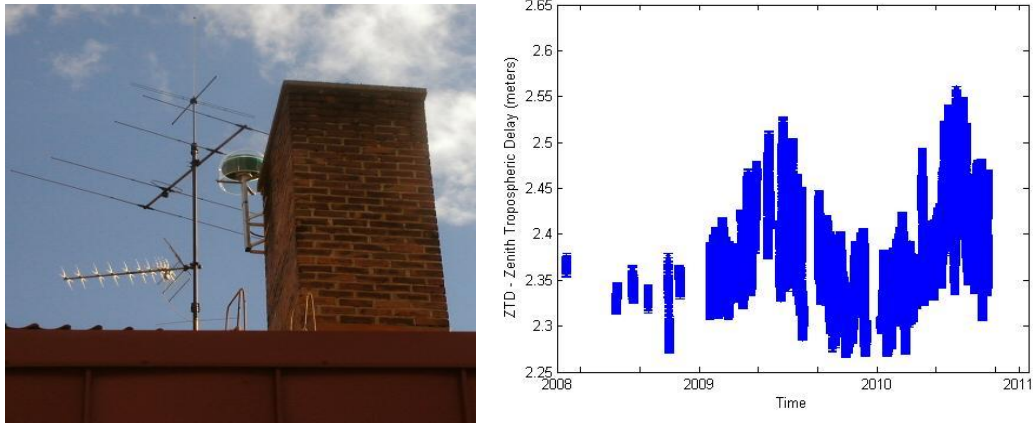


Figure 33: Vindeln station (left), Zenith Tropospheric Delay (right)

This station was built in the city Vindeln on roof top in the residential area in 2006. It is located at LAT 64.202° , LON 19.714° and height 218.09 meters above ground. Figure 33 shows the last three years trend in ZTD (in meters) with Figure 34 shows its corresponding ZHD and ZWD trends (also in meters). Mean residuals (in cm) are plotted with respect to both elevation and azimuth angles (in degrees), as shown in Figure 35. Residuals plot shows some reflections blockages at some clear directions which are mainly due to the other surrounding antenna that are build over it.

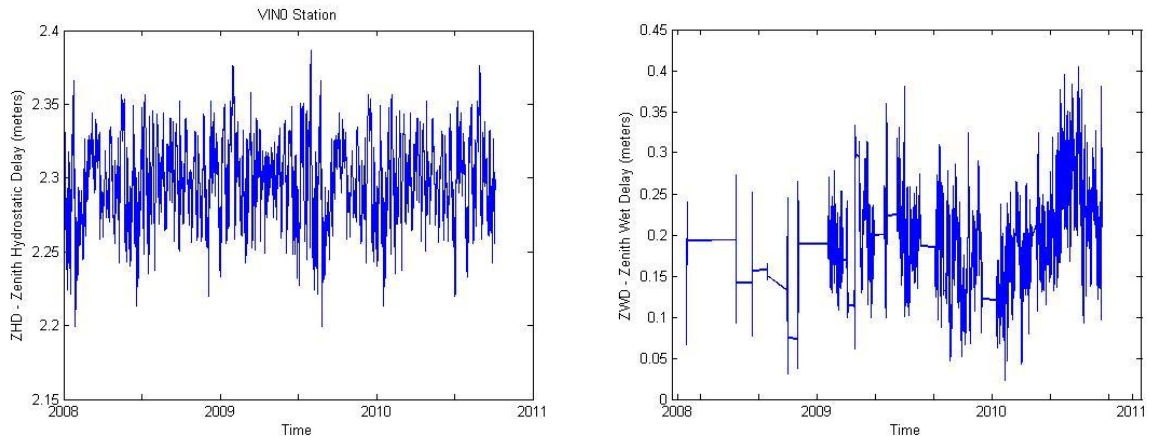


Figure 34: Zenith Hydrostatic Delay plot (left) and its corresponding Zenith Wet Delay plot (right)

Figure 33 and Figure 34 of the ZTD and ZWD plots shows some gaps at different epochs. The gaps in the end after September 2010 are due to the unavailability of the data and the other gaps are due to having some difficulties with the data itself which makes it even hard to process for the GIPSY script. ZTD and ZWD plots are based on the GIPSY software package and cannot be plotted through models due to the rapid change in the atmosphere. On the other hand, the ZHD plot of Figure 34 show a continuous plot which is based on the model that depends on only station surface pressure, station height and the latitude.

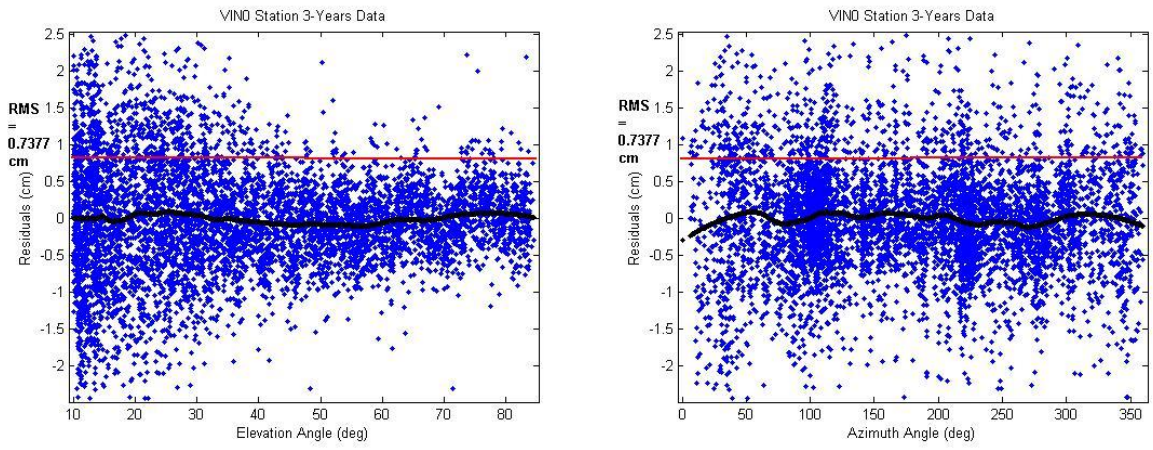


Figure 35: VindelIn station Residual plot as an angle of Elevation angle (left) and as an angle of Azimuth angle (right). Black line is the trend; red line is the root mean square

7 Comparison and Validation with Independent Data sets/ Other Models

Climate models are the numerical representation of the various parts of the earth's climate systems. Similarly GNSS climate models are very good source to measure Tropospheric delay as it has the tendency to work in almost all weather scenarios. It is also a very good source for climate research these days.

7.1 Climate Models

In this section, we did the comparison of selected SWEPOS stations over the three year period with the two other independent climate models for validation of the results. The two most product able widely used climate model in many countries are the ECMWF and RCA models.

7.2 ECMWF

ECMWF – European Center for Medium Range Weather Forecasting Model is an independent organization supports 34 states including major 18 European states, based in London in the United Kingdom. ECMWF was formed in 1975 with few member states with main purpose is to provide medium range weather models for forecasting and now their medium range models can forecast weather for up to 20-days. Their models have been used to reanalyze obtained data from balloons, radiosondes, scatterometers, buoys, satellites and aircrafts. Its basic document is its convention which defines its objectives and the functions of its council.

7.3 RCA Model

RCA – Rossby Center Atmospheric Model is developed and run by SMHI – Swedish Meteorology and Hydrological Institute. It is also known as the regional model. Its main focus is to provide regional climate scenarios specifically for the Nordic region.

7.4 Comparison with Climate Models

7.4.1 ALB0

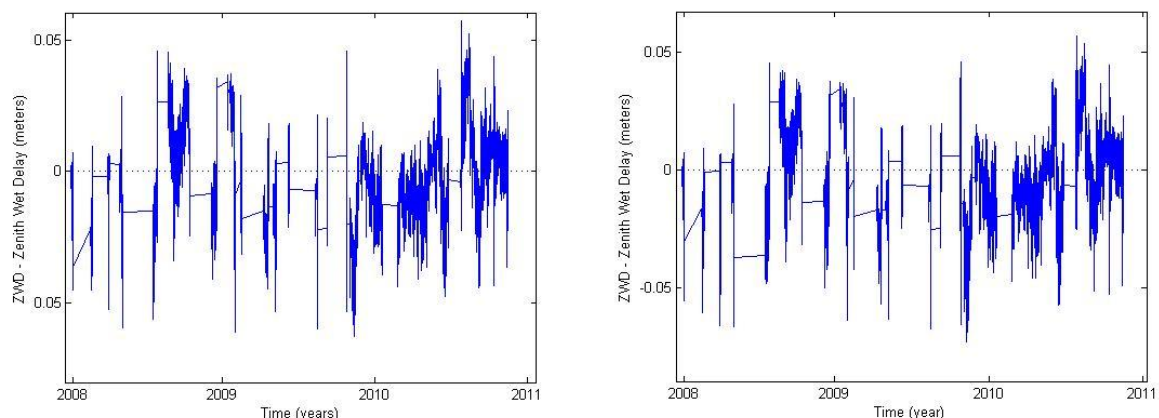


Figure 36: Älvsbyn station comparison plot with ECMWF (left), Comparison with RCA (right). Dotted line is the zero axes

Figure 36 shows the comparison of GIPSY computed solutions versus two independent models ECMWF and the RCA model. The average mean from both the models are between ± 0.05 meters over the last three years, which is very agreeable with no biasing from the models. A better agreement is given from ECMWF with smaller difference. The dotted line shows the zero axes. The average mean difference is 4.1 mm from ECMWF and 4.6 mm from RCA model. And the Standard deviation difference of 6.2 mm with ECMWF and 7.1 mm with RCA model.

7.4.2 GRY0

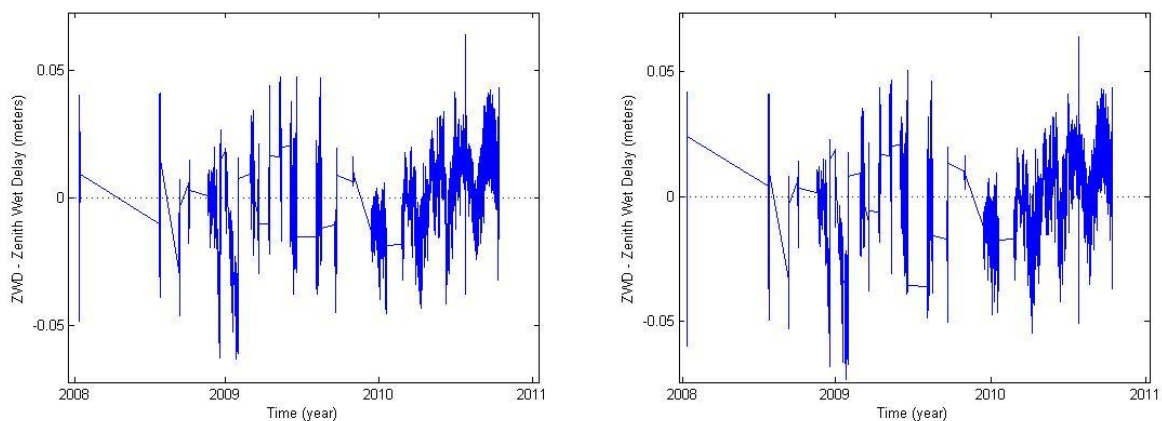


Figure 37: Gryt station comparison plot with ECMWF (left), Comparison with RCA (right). Dotted line is the zero axes

The comparison of GIPSY computed solutions are shown versus two independent model in Figure 37. The average mean from both the models are between ± 0.05 meters over the last three years, which is very good. Here the average mean difference is 1.6 mm from ECMWF and same from RCA model as well. And the Standard deviation difference of 6.6 mm with ECMWF and 6.7 mm with RCA model. A better agreement is given from RCA model with smaller differences compare to ECMWF. The negative part in the plot shows that the obtained/calculated wet delay

is less than the predicted which means this station is working very well and providing the best observations because the more negative the better it works.

7.4.3 HISO

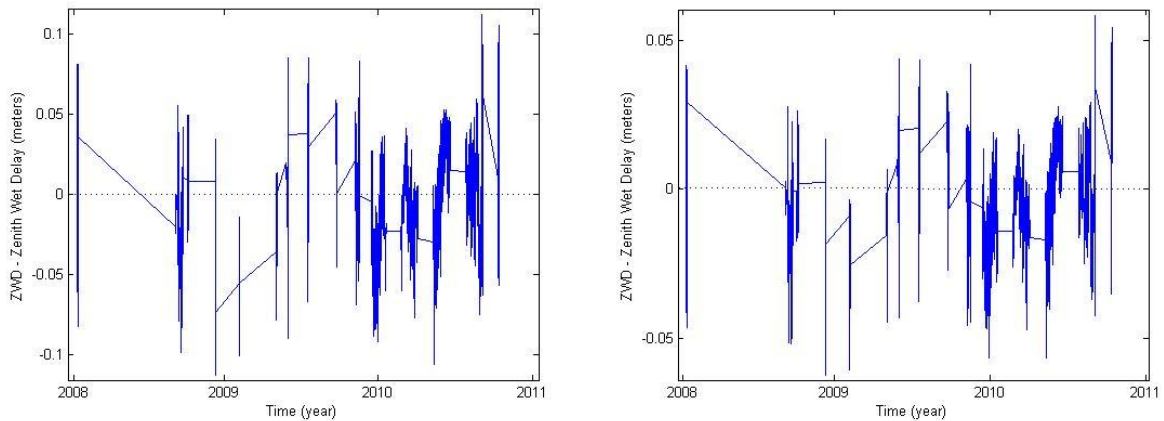


Figure 38: Hisingsbacka station comparison plot with ECMWF (left), Comparison with RCA (right). Dotted line is the zero axes

Figure 38 shows the comparison of GIPSY computed solutions versus two independent models ECMWF and the RCA model. The average mean from RCA the model is between ± 0.05 meters and around ± 0.1 meters from ECMWF, which is very agreeable. A better agreement is given from RCA with smaller difference. The dotted line shows the zero axes. The average mean difference is 3.1 mm from ECMWF and 3.0 mm from RCA model. And the Standard deviation difference of 6.2 mm with ECMWF and 6.3 mm with RCA model. The negative part in the plot shows that the obtained/calculated wet delay is less than the predicted which is very good trend for the observation.

7.4.4 NYBO

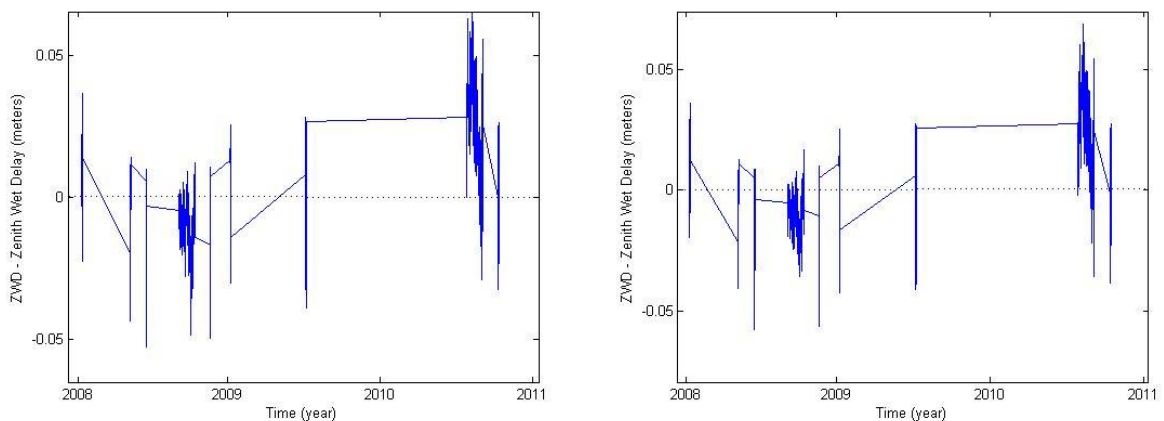


Figure 39: Nyborg station comparison plot with ECMWF (left), Comparison with RCA (right). Dotted line is the zero axes

Figure 39 shows the comparison of GIPSY computed solutions versus two independent models. The average mean from both the models are between ± 0.05 meters over the last three years, which is very good. Here the average mean difference is 4.2 mm from ECMWF and also the same

with RCA model. And the standard deviation difference of 6.8 mm both with ECMWF and with RCA model. A better agreement is given from RCA model with smaller differences compare to ECMWF. The negative part in the plot shows that the obtained/calculated wet delay which is less than the predicted (and positive part shows the opposite), means this station is working very well and providing the best observations.

7.4.5 OVT0

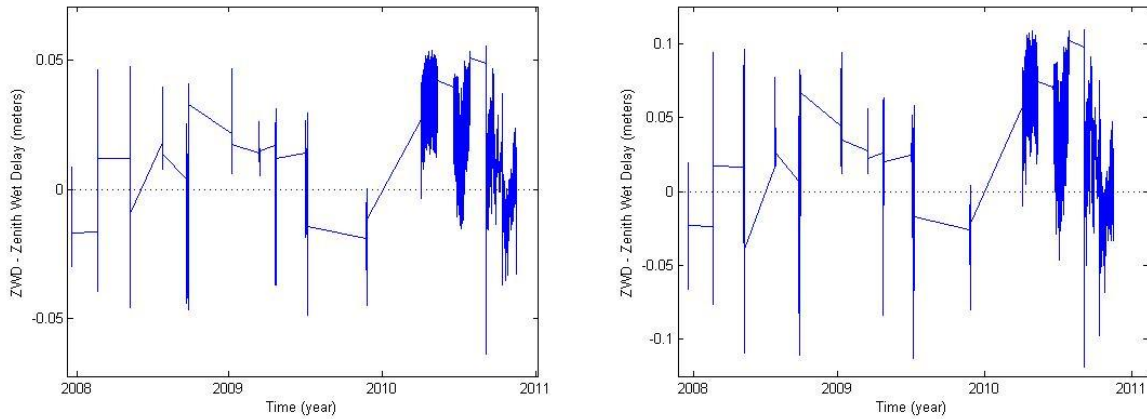


Figure 40: Övertorneå stations comparison plot with ECMWF (left), Comparison with RCA (right). Dotted line is the zero axes

The comparison of GIPSY computed solutions are shown versus two independent model in Figure 40. The average mean from ECMWF is between ± 0.05 meters and ± 0.1 meters from RCA, over the last three years duration, which is very good. Here the average mean difference is 3.2 mm from ECMWF and same from RCA model as well. And the Standard deviation difference of 7.1 mm with ECMWF and 7.0 mm with RCA model. A better agreement is given from ECMWF model with smaller differences compare to RCA model. The negative part in the plot shows that the obtained/calculated wet delay is less than the predicted which means this station is working very well and providing the best observations because the more negative the better it works.

7.4.6 OXE0

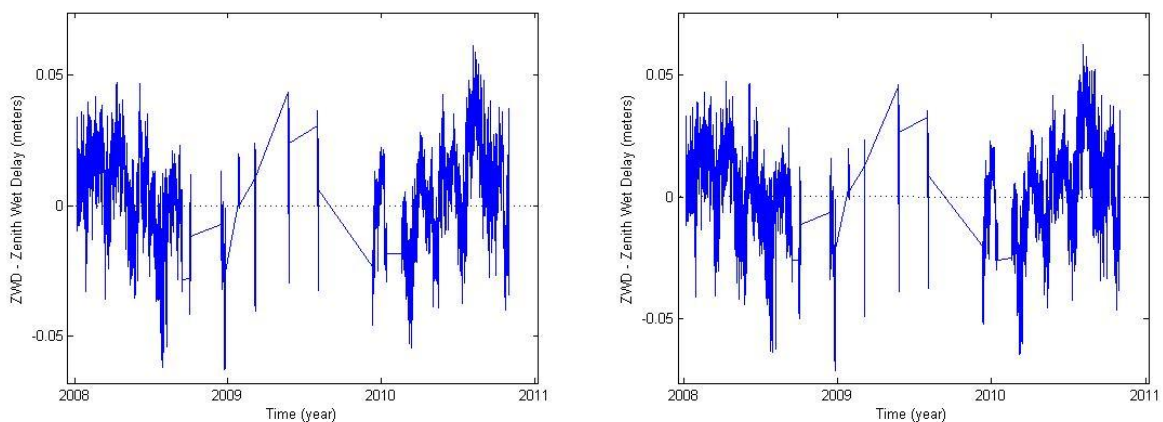


Figure 41: Oxelösund station comparison plot with ECMWF (left), Comparison with RCA (right). Dotted line is the zero axes

The comparison of GIPSY computed solutions are shown versus two independent model in Figure 41. The average mean from both the models are between ± 0.05 meters over the last three years, which is very agreeable and not biasing from any model. Here the average mean difference is 1.3 mm from ECMWF and 1.2 mm from RCA model as well. And the Standard deviation difference of 7.4 mm with ECMWF and 7.5 mm with RCA model. A better agreement is given from RCA model with smaller differences compare to ECMWF. The negative part in the plot shows that the obtained/calculated wet delay is less than the predicted (and positive part shows the opposite) which means this station is working very well and providing the best observations because the more negative the better it works.

7.4.7 STA0

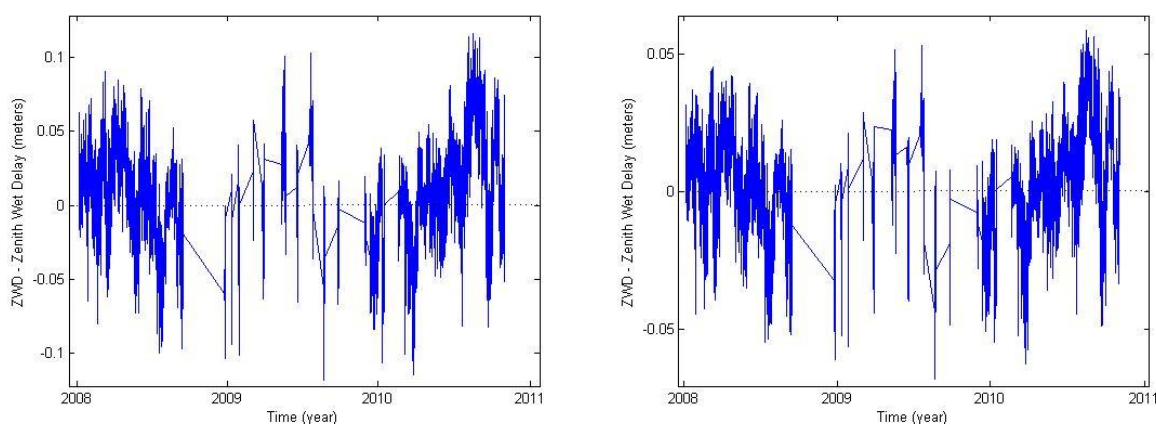


Figure 42: Stavsnäs station comparison plot with ECMWF (left), Comparison with RCA (right). Dotted line is the zero axes

Figure 42 shows the comparison of GIPSY computed solutions versus two independent models ECMWF and the RCA model. The average mean from RCA the model is between ± 0.05 meters and ± 0.1 meters from ECMWF, which is very agreeable with no biasing from the models. A better agreement is given from RCA with smaller difference. The dotted line shows the zero axes. The average mean difference is 1.3 mm from ECMWF and 1.2 mm from RCA model. And the Standard deviation difference of 6.7 mm with ECMWF and 6.9 mm with RCA model. The negative part in the plot shows that the obtained/calculated wet delay is less than the predicted (and positive part shows the opposite) which is very good trend which means that this station is working very well and providing the best observations because the more the negative the better it works.

7.4.8 VASO

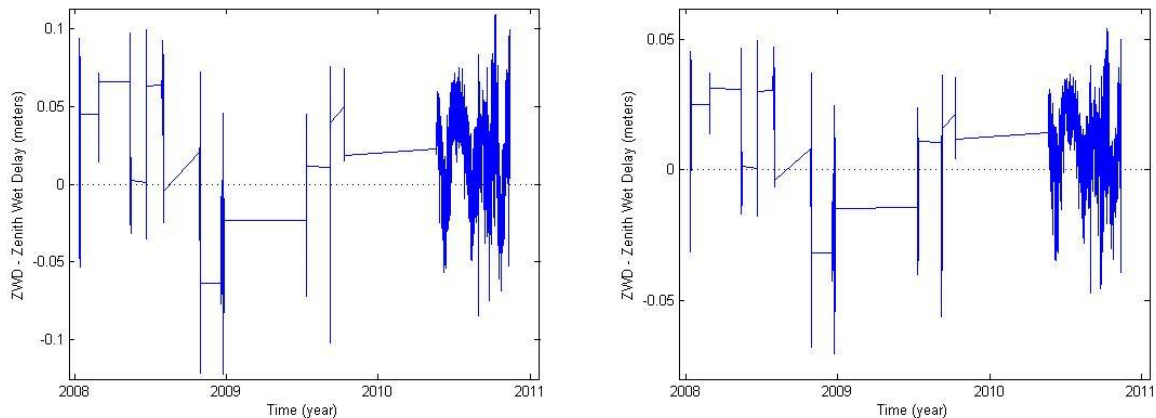


Figure 43: Västerås station comparison plot with ECMWF (left), Comparison with RCA (right). Dotted line is the zero axes

The comparison of GIPSY computed solutions are shown versus two independent model in Figure 43. The average mean from ECMWF is between ± 0.1 meters and ± 0.05 meters from RCA, over the last three years duration, which is very good. The RCA model gives better agreement than ECMWF model. Here the average mean difference is 1.8 mm from ECMWF and same from RCA model as well. And the Standard deviation difference of 8.0 mm with ECMWF and also the same with RCA model. The negative part in the plot shows that the obtained/calculated wet delay is less than the predicted which means this station is working very well and providing the best observations because the more negative the better it works.

7.4.9 VINO

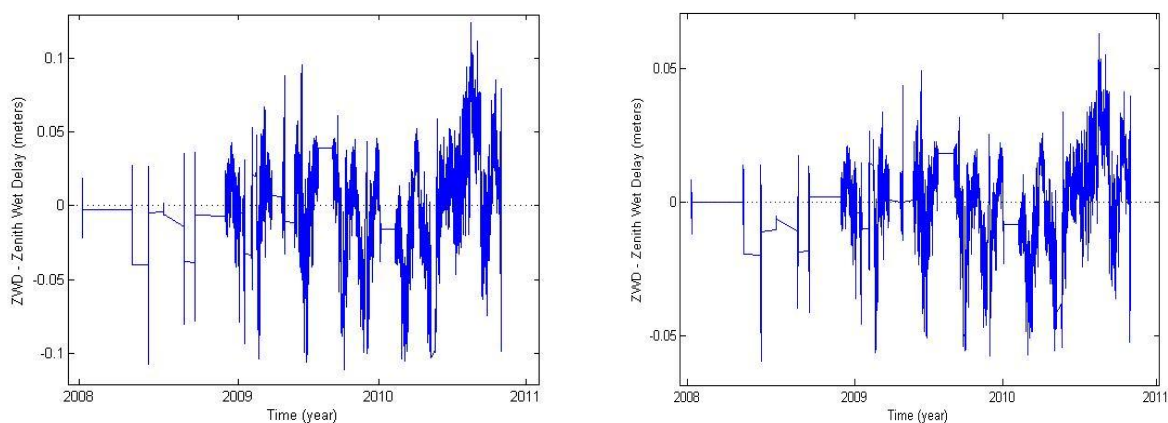


Figure 44: Vindeln station comparison plot with ECMWF (left), Comparison with RCA (right). Dotted line is the zero axes

The comparison of GIPSY computed solutions are shown versus two independent model in Figure 44. The average mean from ECMWF model is between ± 0.1 meters and ± 0.05 meters over the last three years duration, which is very good and agreeable value. Here the average mean difference is 2.4 mm from ECMWF and 1.5 mm from RCA model. And the Standard deviation

difference of 6.4 mm with ECMWF and also the same with RCA model. A better agreement is given from RCA model with smaller differences compare to ECMWF. The negative part in the plot shows that the obtained/calculated wet delay is less than the predicted which means this station is working very well and providing the best observations.

8 Error Sources

8.1 Ionosphere Propagation Path Delay

Ionospheric propagation path delay of microwave signal depends on its frequency which means the lower the frequency the greater the delay and vice versa i.e. L2 ionospheric delay is greater than L1. It usually arises from the ionized atmosphere or the TEC (total electron content) present along the path which means ionospheric delay is proportional to the TEC which is present at an altitude of 100 to more than 1000 Km (see Figure 45) however TEC depends on number of important factors,

- The 11-year solar cycle or solar magnetic activity is the electron density level from sun reaches maximum after every 11-years which correspond to peak in the solar flares activity
- The geographic location because the electron density level are minimum in mid-latitudes and uncertain at the polar and equatorial regions
- The time of day due to the electron density reaches maximum in early afternoon and minimum around midnight
- The time of year because the electron density level reaches maximum in winter and minimum in summer

Scintillation is an effect similar to the twinkling of stars resulting in rapid fluctuations of signal strength results from the light ray bending as they pass through the inhomogeneous atmosphere or in other words it occurs due to the result of variations in refractive index. It increases in the daytime due to solar activity and opposite in the night. Scintillation effect is inversely proportional to the square of the operating frequencies and is predominant in lower microwave frequencies typically below 4GHz and is independent of the elevation angle.

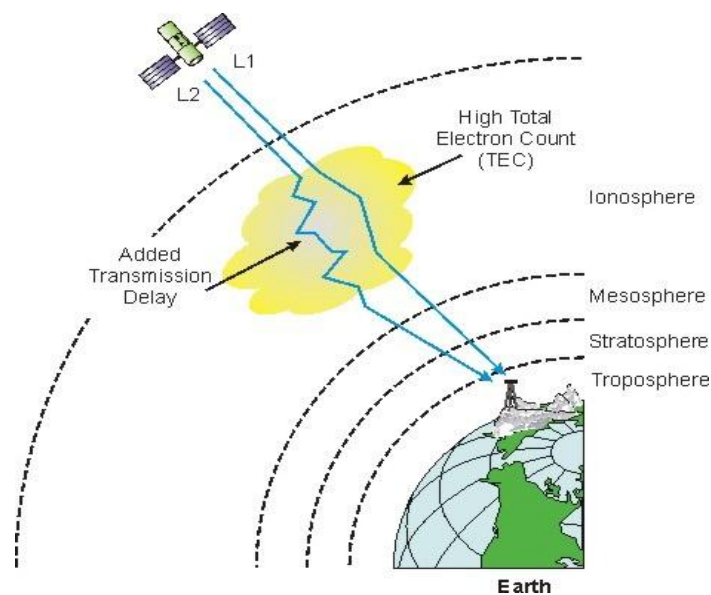


Figure 45: Ionospheric delay error sources⁷

⁷ <http://www.wirelessdictionary.com/Wireless-Dictionary-Ionospheric-Delay-Definition.html>

Another important phenomenon in the ionosphere is dispersion which usually degrades the signal over long distances. Dispersion often describes for the light waves but it could possibly occur for any kind of waves. The effect of Ionospheric changes slowly and can be averaged over time.

8.2 Tropospheric Propagation Path Delay

Troposphere is an electrically neutral, non dispersive medium for radio frequencies below 15 GHz at an altitude of 10 Km above earth's surface. Unlike the Ionospheric propagation path delay, the Tropospheric propagation path delay can't be easily removed by combining L1 and L2 observations mainly because it is independent of frequency. This is a region where weather activity occurs.

Humidity is one of the major error sources in troposphere and on top of that it is independent of frequency. Several other significant effects on communication are refraction, attenuation and depolarization. Errors in Tropospheric are more difficult than Ionospheric errors.

Atmospheric attenuation is caused by the molecules and by rain. Rain has very dramatic effects in communication which leads to poor observations. The attenuation is caused by the combination of absorption and scattering. The magnitude of attenuation depends upon the size of the rain drops compared to the wavelength of the radio waves: the attenuation increases rapidly with the frequency in the microwave region. It should also be noted that everything that absorb radio wave also contributes noise.

Refraction by the neutral atmosphere causes a slight shift in apparent elevation of a satellite as seen from a ground station. Refraction effect increases with elevation.

Depolarization is caused by the fact that rain drops are not exactly spherical but slightly flattened. It can be of importance when frequency reuse is employed.

8.3 Receiver related errors

Sometime using different receiver from different manufacturers also may cause disruption in the observation of GNSS applications due to the limitation to remove multipath errors at all elevation angle because of the dependence on different frequency range, when using many brand receiver simultaneously.

8.4 Satellite ephemeris errors

Satellite positions as a function of time, which are included in the broadcast satellite navigation message, are predicted from previous satellite observations at the ground control stations. Typically, overlapping 4-hour data spans are used by the operational control system to predict post satellite orbital elements for each 1-hour period. As might be expected, modeling the forces acting in the satellite will not in generally is perfect which causes some errors in the estimated satellite positions, known as ephemeris errors. It is usually in the order of 2 to 5 meter and can possible reach up to 100 meters under selective availability (SA), but this feature is currently disable in GPS satellites and only government and military can use it with special military GPS receivers.

Satellite ephemerides contain information about the location of a satellite at any given time. In the case of positioning of satellite, ephemerides contains information consists of Keplerian parameters at a certain epoch, rate of change of these elements, clock information and clock correction terms. Accurate ephemerides information is required for location precise positioning on earth.

8.5 Satellite Geometry

The various error types are discussed in section that affects the accuracy of the satellite position. However, these are not the only factors; the satellite geometry which represents the geometric locations plays an important role in total positioning accuracy. Good satellite geometry is obtained when satellites are spread out in the sky as shown in the Figure 46.

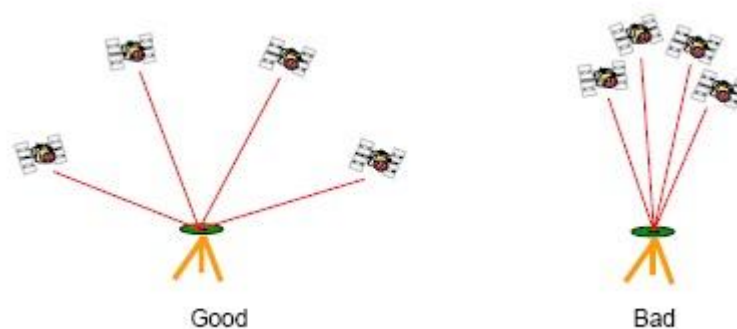


Figure 46: Good and Bad DOP due to Satellite Geometry⁸

The satellite geometry effect can be measured by a single dimensionless number call dilution of precision (DOP) which indicates the quality of satellite geometry. Low DOP means good geometric strength and vice versa. DOP is computed based on the receiver-satellite geometry at any instance with known satellite coordinates.

8.6 Satellite Orbit and Clock Errors

Atomic clocks onboard satellites are very expensive. They are good but not great and still they are not good enough. Also the GPS system itself has limitations in its orbit and clock parameters and needs to be updated quite often.

8.7 Communication Errors

Communication error or signal arrival time error occurs sometime during the communication when the transmitter and receiver of satellite and ground station are not synchronized properly. It is also happens sometime due to the bad weather conditions. The position calculated by satellite receiver requires current time which also causes communication errors when not defined properly.

⁸ http://www.papyrus.co.il/FAQ/dilution_of_precision.htm

8.8 Space Weather Errors

Space weather refers to the changing conditions in the space environment (outside the Van Allen radiation belts around Earth's atmosphere which are at an altitude of 13000 to 60000 Km above Earth's surface) due to the solar wind and coronal mass ejection (CME) which is solar flares and large plasma clouds thrown out from the sun, see Figure 47. Space weather has a direct influence on satellites and their performance which drastically enhances the problems in GPS satellites' electronic onboard.



Figure 47: Space weather errors due to the solar activity and ejection of solar flares⁹

8.9 Atmospheric Drag

Atmospheric drag varies in magnitude with the solar cycle. During high solar activity, the outer layers of the atmosphere are heated and expand, leading to large drag on satellites, especially for those in low Earth orbit (LEO), which may cause damage to the satellite and disrupt communication.

8.10 Radio Blackouts

It is caused by the ionized air or plasma created around spacecraft due to heat from the friction against the atmosphere. Radio blackout lasts for several minutes. It causes misunderstanding of data at the right epoch and also decreases the accuracy for navigation satellites.

8.11 Antenna Phase Center variations

It is well known that a physical satellite antenna doesn't have a phase center, but in theory it is the point of an antenna at which a satellite signal is received or transmitted. This point is not a fixed point in the antenna but a point that varies in location depending on the frequency and direction of the incoming signal. The antenna phase center varies with elevation and azimuth of the satellite antenna as well as the intensity of the observed signal. As a result, additional range error can be expected. This error also depends on the antenna type and is typically about a few centimeters. Due to its small size, this error is almost neglected in most of the practical GNSS applications.

⁹ <http://www.land-of-kain.de/docs/spaceweather/>

8.12 Multipath Effects

Multipath is a major error source caused by the reflection of satellite signal on surrounding objects like building, trees, hills etc and arrives at receiver antenna through many paths and at different intervals. The straightforward method to reduce this effect is to use the measurement of the station that don't have any reflecting object in its surrounding also by using choke ring antenna (see Figure 48), with microwave absorber below or around the antenna greatly reduce the strength of backscattered radiation and multipath signals.



Figure 48: Choke Ring Antenna (Image courtesy Trimble)¹⁰

8.13 Gaseous Absorption

Electromagnetic energy gets absorbed and converted into heat due to gaseous absorption as it passes through the troposphere. The absorption is primarily due to the presence of uncondensed water vapor. Presence of free electrons in the atmosphere also causes absorption due to collision of electromagnetic waves with these electrons. Absorption increases with a decrease in elevation angle. Absorption is also observed to increase with humidity.

8.14 Site-dependent Effects

Apart from number of error source in GNSS applications, some local error source related to specific station could also cause a big difference in the satellite observations and is a major error source. Some of the site-dependent errors are due to antenna, radome, station design and the local environment. Among these the connecting cable are major sources to instrumental errors. The different antenna designs, different radome designs, cables, receivers and equipment could also be the major site dependent error sources. Also the local environment like site surrounded by trees, hills, terrain of local environment, forest, vegetation and other close objects changes the characteristics of antenna and sometime blockage of signal resulting in cycle slips which leads to the weaker satellite constellation measurement at that epoch.

¹⁰ <http://www.trimble.com/infrastructure/gnss-choke-ring-antenna.aspx?dtID=overview>

9 Conclusion

The amount of water in the earth's atmosphere is dependent on evaporation and condensation which vary with the temperature and temperature is correlated to the moisture. This study focuses on the error source on the ground and changes in the Tropospheric water vapor content

In this thesis, we have seen many different situations with the randomly selected 9-geodetic network stations over the three year period including all seasonal activities and variations. We have also seen other factors like site under the influence of another antenna, high latitude and mid-latitude effects, blockage due to the presence of an object or a building, multipath effects, side-dependent effects, surrounding electromagnetic environment of the GNSS antenna etc. We have also seen the mean residuals of every station as an angle of Azimuth and Elevation angle for error sources.

We have also computed the root mean square of every station which is about 6mm on average (see Table 3). The average mean difference of GIPSY computed solution verses the two independent data sets are between 1 – 4mm. Standard deviation of difference of every station with the two climate models are between 6 – 8mm on average.

Station ID	RMS (mm) SWEPOS Stations	Mean Difference (m)		Standard Deviation(m)	
		ECMWF	RCA	ECMWF	RCA
ALBO	5.829	0.0041	0.0046	0.0062	0.0071
GRYO	5.428	0.0016	0.0016	0.0066	0.0067
HISO	5.676	0.0031	0.0030	0.0062	0.0063
NYBO	5.673	0.0042	0.0042	0.0068	0.0068
OVT0	5.275	0.0032	0.0032	0.0071	0.0070
OXEO	6.938	0.0013	0.0012	0.0074	0.0075
STA0	7.095	0.0013	0.0012	0.0067	0.0069
VASO	7.095	0.0018	0.0018	0.0080	0.0080

VINO	7.377	0.0024	0.0015	0.0064	0.0064
------	-------	--------	--------	--------	--------

Table 3: Shows the RMS of every station, Mean difference of GIPSY computed solution with two climate models and the standard deviation of difference of the GIPSY computed solution with the two independent climate models

Till year 2010, only 25 first-stations were used for measuring Tropospheric delay measurement but after these results and validation we can conclude that these nine second-order stations could also be usable for measuring Tropospheric delay estimation. One of the biggest advantages of using this technique is it is very cheap compare to the much expensive balloon and airborne techniques and is based on the existing infrastructure. Secondly GNSS measurements can be obtained at anytime and in any weather condition known demand. For more sophisticated measurement we can use balloons and airborne systems and for launching those system needs a proper planning as these systems are launched only few time per year whereas GNSS systems work 24/7 and in all weather conditions. So from all the results shown in this thesis we can say that these second order stations are definitely usable for monitoring Tropospheric water vapor activity and delay estimation.

10 Future Work and Recommendation

In future, we definitely need to take several years of data for more accurate measurement and estimation. Other more than 150 second-orders needs to be tested for the same purpose. Systematic effects will also need to be studied in order to obtain more accurate and realistic trends with very small uncertainties and fewer errors.

Use of GLONASS and GALILEO frequency or other GNSS systems to see how geodetic station behaves with different frequencies and different GNSS systems, other than GPS based GNSS system. Site-dependent effects are very crucial and must be considered and given more priority. Use choke ring antenna on every site with absorber to reduce the effect of multipath.

Use of other GNSS based systems also plays an important role in the positioning and navigation, more different satellite navigation systems means more frequencies, works on several different packages at the same time, would increases the data accuracy tremendously in terms of realistic calculations and predictions. Also more software packages needs to be developed to work more efficiently.

Behavior of these geodetic stations with other software and packages needs to be done to understand the effects of local atmosphere and local error more in depth. Computer models needs to be defined in a more sophisticated way to get deeper understanding about the how the atmosphere with varying atmospheric conditions effects the signal propagation.

Bibliography

- Bevis, M., S. Chriswell, T. A. Herring, R. A. Anthes, C. Rocken, and r. H. Ware, (1994), GPS Meteorology: Mapping Zenith Wet Delays onto Precipitable Water, *J. Appl. Meteorol.*, 33, 379 – 386
- Cardillo, P., (2007), Near Real Time GNSS processing for monitoring of EPN station performance, reference frames and weather prediction, *Master Thesis*, Chalmers University of Technology, Sweden
- Egziabher, D. G., and Gleason, C., (2009), *GNSS Applications and Methods*, Artech house, Boston
- Ekström, M., (2008), Satellite Measurements of upper Tropospheric water, *Ph.D Thesis*, Chalmers University of Technology, Sweden
- Elosegui, P., J. L. Davis, R. T. K. Jaldehag, J. M. Johansson, A.E. Niell, and I. I. Shapiro, (1995), Geodesy using the Global Positioning System: the effects of signal scattering on estimated of site position, *J. Geophys. Res.*, 100, B6, 9921 – 9934
- Emardson, T. R., and Derks H. J. P., (1999), On the Relation between the Wet Delay and the Integrated Precipitable Water Vapor in the European Atmosphere, *Meteorol. Appl.*, 6, 1–12
- Emardson, T. R., G. Elgered and J. M. Johansson, (1998), Three months of continuous monitoring of atmospheric water vapor with a network of Global Positioning System receivers, *J. Geophys. Res.*, 103. 1807–1820
- Emardson. T. R., Johansson J. M., and Elgered G., (2000), The systematic behavior of Water Vapor estimates using four years of GPS observations, *Trans. IEEE Geosci. Remote Sens.*, 38, 324–329
- Foelsche, U., Kirchengast, G., and Steiner, A., (2006), *Atmosphere and Climate studies by Occultation Methods*, Springer, Netherlands
- Granström, C., (2006), Site dependent effects in high accuracy applications of GNSS, *Licentiate Thesis*, Chalmers University of Technology, Sweden
- IGS, (2004), IGS – International GNSS Service, available from <http://igs.cb.jpl.nasa.gov>, (April 2011)
- Inside GNSS, (2011), Inside GNSS Magazine, April – November Issue, available from <http://www.insidegnss.com/magazine>. (Nov 2011)
- Iran, P. S., (2006), Statistical Analysis of Tropospheric Wet Delay gradients derived from VLBI and GPS, *Master Thesis*, Chalmers University of Technology, Sweden
- Jaldehag, R. T. K., Johansson J. M., Rönnäng B.O., Elosegui P., Davis J. L., Shapiro I.I., and Niell, A. E., (1996), Geodesy using the Swedish Permanent GPS Network: effects of signal scattering on estimated of relative site positions, *J. Geophys. Res.*, 101, B8, 841–860
- Jahnberg, A., and Jonsson, B., (2003), A System for removal of Snow at SWEPOS-stations, *Master Thesis*, Chalmers University of Technology, Sweden

- Johansson, J. M., Emardson T. R., Jarlemark P. O. J., Gradinarsky L. P., and Elgered G., (1998), The Atmospheric influence on the results from the Swedish GPS Network, *Physics and Chemistry of the Earth*, 23, 107–112
- Jones, c., U. Willen, A. Ullerstig, and U. Hansson, (2004), The Rossby Centre regional atmospheric climate model part I: Model climatology and performance for the present climate over Europe. *Ambio*, 33: 4–5, 199–210
- Löfgren, J. S., (2011), Observing Sea Level using reflected Global Navigation Satellite System signals, *Licentiate Thesis*, Chalmers University of Technology, Sweden
- Maini, A. K., and A. V., (2010), *Satellite Technology: Principles and Applications*, 2nd Edition, Wiley, UK
- Nilsson, T., and G. Elgered, (2008), Long- term trends in the atmospheric water vapor content estimated from ground-based GPS data, *J. Geophys. Res.*, 113, D19101, doi : 10.1029 / 2008JD010110
- Nilsson, T., (2008), Measuring and Modeling variations in the distribution of atmospheric water vapor using GPS, *Ph.D Thesis*, Chalmers University of Technology, Sweden
- Ning, T., (2010), Global Navigation Satellite System: Applications with Time Scales from Seconds to Decades, *Licentiate Thesis*, Chalmers University of Technology, Sweden
- Ning, T., G. Elgered, and J.M. Johansson, (2011), The Impact of Microwave Absorber and Radome Geometries on Geodetic Measurements with Ground-Based GNSS Antennas, *J. Adv. Space. Res. Scientific Applications of Galileo and Other Global Navigation Satellite Systems*, 47(2), pp. 186 – 196
- Pramualsardikul, S., (2007), GPS measurements of Atmospheric water vapor in a low-latitude region, *Licentiate Thesis*, Chalmers University of Technology, Sweden
- Ross, R. J., and W. P. Elliott, (1996), Tropospheric water vapor climatology and trends over North America, *J. Climate*, 9:3561–3574
- Seeber, G., (1993), *Satellite Geodesy – Foundations, Methods and Applications*, Walter de Gruyter, Berlin, 532 pp.
- Schuler, T., (2001), On-ground based GPS Tropospheric Delay Estimation, Ph.D Thesis, Bundeswehr University, Germany
- SWEPOS, (2005), SWEPOS – A National Network of Reference Stations for GPS, available from http://swepos.lmv.lm.se/english/index_swepos.htm, (April 2011)
- Teunissen, P. J. G., and A. Kleusberg, (1998), *GPS for Geodesy*, 2nd Edition, Springer, Berlin
- Webb F. H., and Zumberge J. F., 1993, An Introduction to the GIPSY/OASIS-II, *JPL Publ.*

Appendix A: List of Tables

Table A.1: RMS, Mean Difference and Standard Deviation of Difference among GIPSY computed solution and Models

Station ID	RMS (mm) SWEPOS Stations	Mean Difference (m)		Standard Deviation(m)	
		ECMWF	RCA	ECMWF	RCA
ALBO	5.829	0.0041	0.0046	0.0062	0.0071
GRYO	5.428	0.0016	0.0016	0.0066	0.0067
HISO	5.676	0.0031	0.0030	0.0062	0.0063
NYBO	5.673	0.0042	0.0042	0.0068	0.0068
OVT0	5.275	0.0032	0.0032	0.0071	0.0070
OXE0	6.938	0.0013	0.0012	0.0074	0.0075
STA0	7.095	0.0013	0.0012	0.0067	0.0069
VAS0	7.095	0.0018	0.0018	0.0080	0.0080
VINO	7.377	0.0024	0.0015	0.0064	0.0064

Table A.2: Chosen SWEPOS GNSS-stations and their details

Station ID	Station Name	Latitude (N) (deg)	Longitude (E) (deg)	Height (meters)	Established Date
ALB0	Älvsbyn	65.67398	21.006935	75.862	2006-06-14
GRY0	Gryt	58.186663	16.800849	53.733	2004-08-20
HIS0	Hisingsbacka	57.732354	11.732354	63.699	2004-10-13
NYB0	Nyborg	66.795913	23.170021	38.416	2006-07-25
OVT0	Övertorneå	66.385718	23.6587	100.582	2006-05-19
OXE0	Oxelösund	58.670953	17.107038	46.758	2002-02-04
STA0	Stavsnäs	59.308861	18.693254	35.902	2001-02-21
VAS0	Västerås	59.64568	16.56136	68.483	1999-03-05
VIN0	Vindeln	64.202226	19.714043	217.959	2006-06-29

Table A.3: Comparison of Four main current GNSS systems

	GPS	GLONASS	Galileo	COMPASS
Affiliation	United States	Russia	Europe	China
Satellites	32	23 (30 with CDMA)	2 + 22 (Budgeted)	10 + 30 (Planned)
Orbital Planes	6	3	3	3
Orbital Height (km)	20200	19100	23222	21150
Orbital Period	11 hr 28 min	11 hr 15 min	14 hr 7 min	12 hr 50 min
Orbital Inclination	55	64.8	58	55.5
Multiple Access	CDMA	FDMA/CDMA	CDMA	CDMA
Carrier Frequency (MHz)	<u>1575.42 (L1)</u> <u>1227.60 (L2)</u> 1381.05 (L3) 1379.91 (L4) 1176.45 (L5)	1598.06 – 1605.38 1242.94 – 1248.63	1164 – 1215 1215 – 1300 1559 – 1592	1561.098 1589.742 1268.520 1207.140
Current Status	Fully Operational	Fully Operational (CDMA in preparation)	Partly Operational	Partly Operational

Appendix B: List of Figures

ALB0:

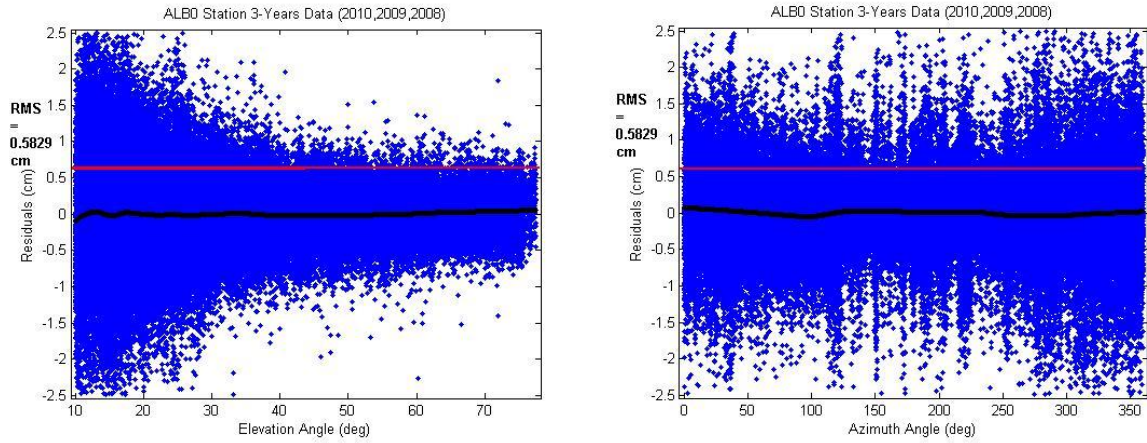


Figure 12: Älvsbyn station Residual plot as an angle of Elevation angle (left) and as an angle of Azimuth angle (right). Black line is the trend; red line is the root mean square

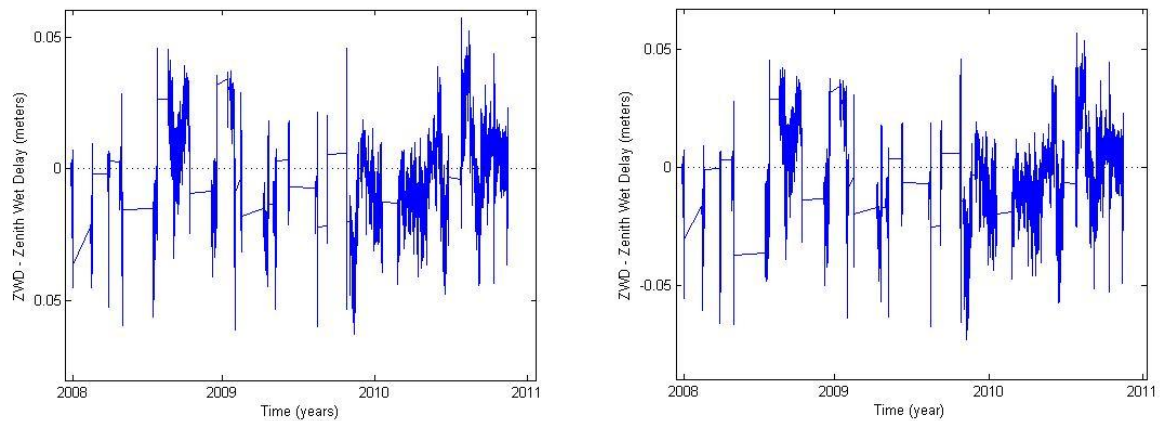


Figure 36: Älvsbyn station comparison plot with ECMWF (left), Comparison with RCA (right). Dotted line is the zero axes

GRY0:

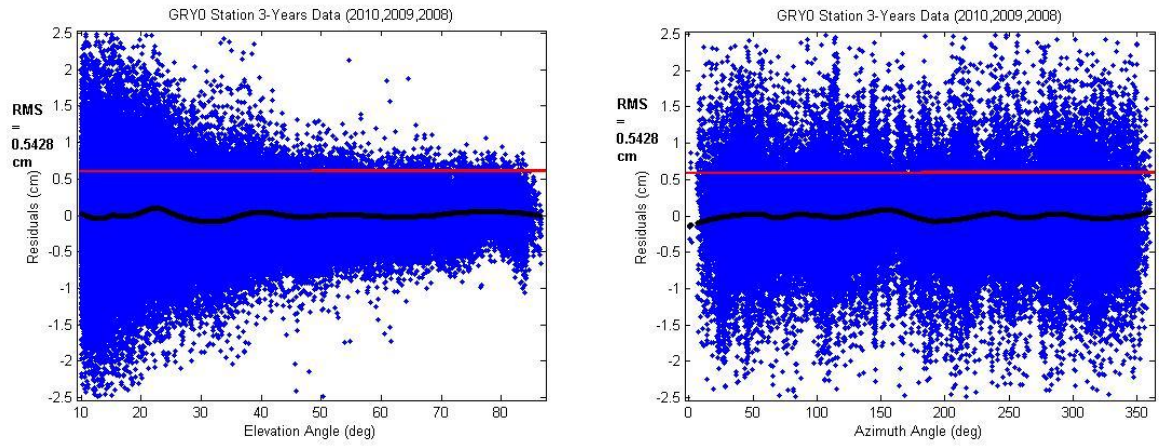


Figure 14: Gryt station Residual plot as an angle of Elevation angle (left) and as an angle of Azimuth angle (right). Black line is the trend; red line is the root mean square

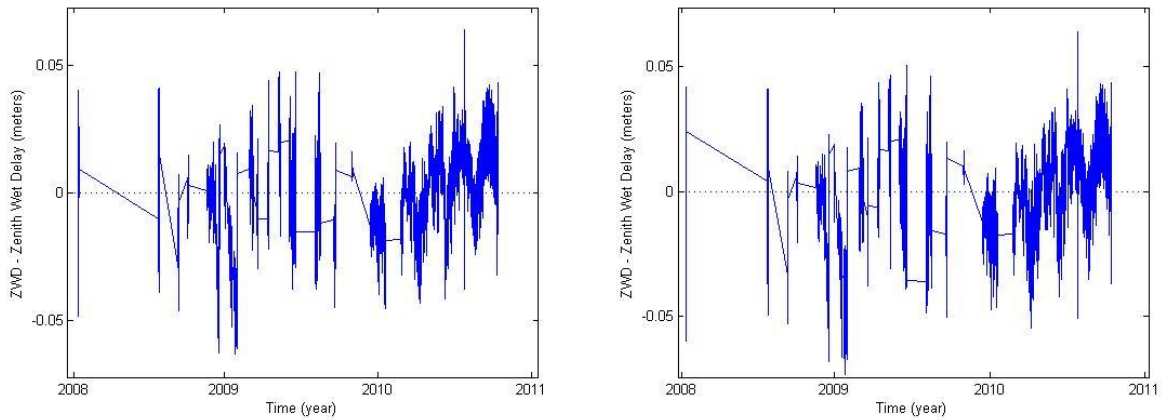


Figure 37: Gryt station comparison plot with ECMWF (left), Comparison with RCA (right). Dotted line is the zero axes

HISO:

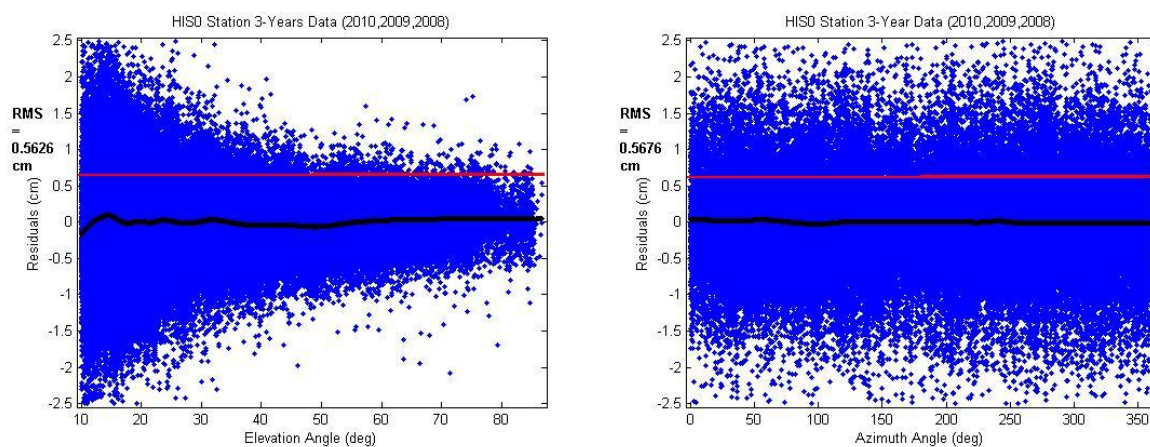


Figure 17: Hisingsbacka station Residual plot as an angle of Elevation angle (left) and as an angle of Azimuth angle (right). Black line is the trend; red line is the root mean square

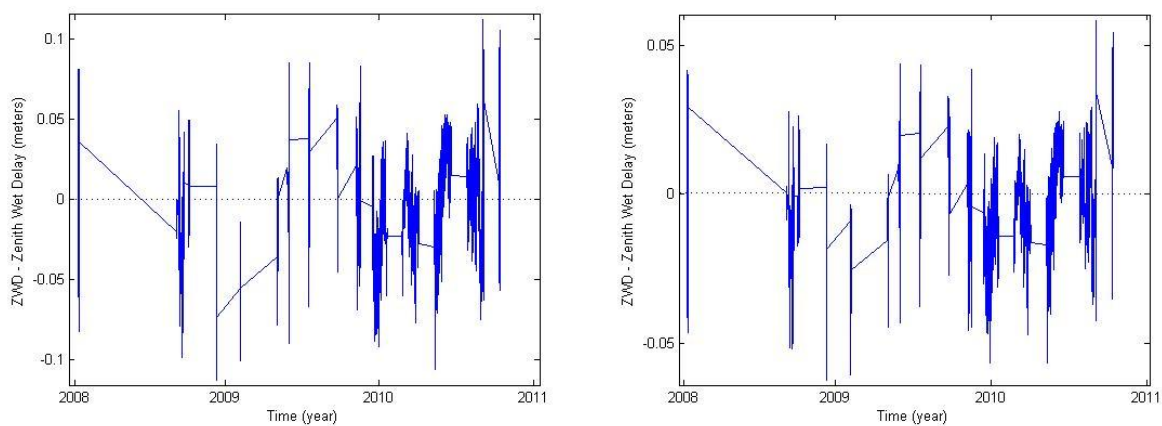


Figure 38: Hisingsbacka station comparison plot with ECMWF (left), Comparison with RCA (right). Dotted line is the zero axes

NYBO:

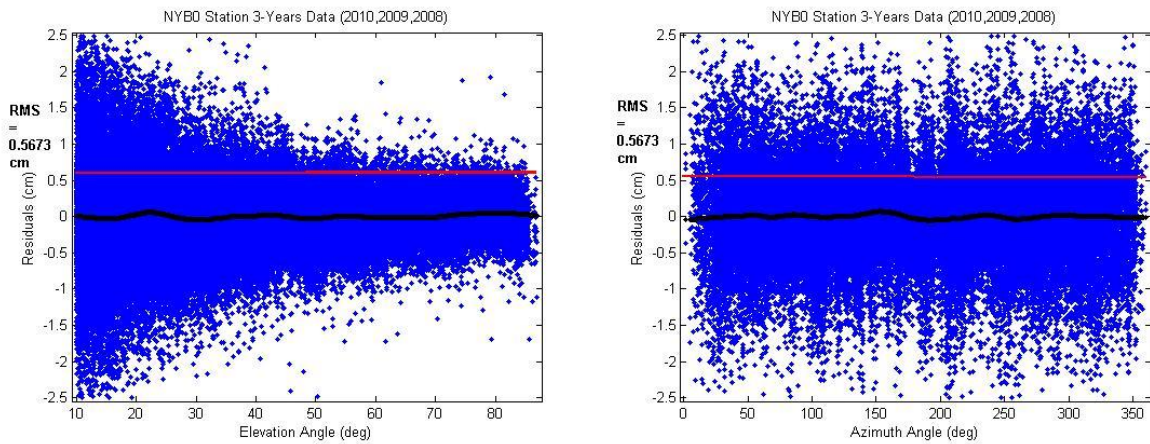


Figure 20: Nyborg station Residual plot as an angle of Elevation angle (left) and as an angle of Azimuth angle (right). Black line is the trend; red line is the root mean square

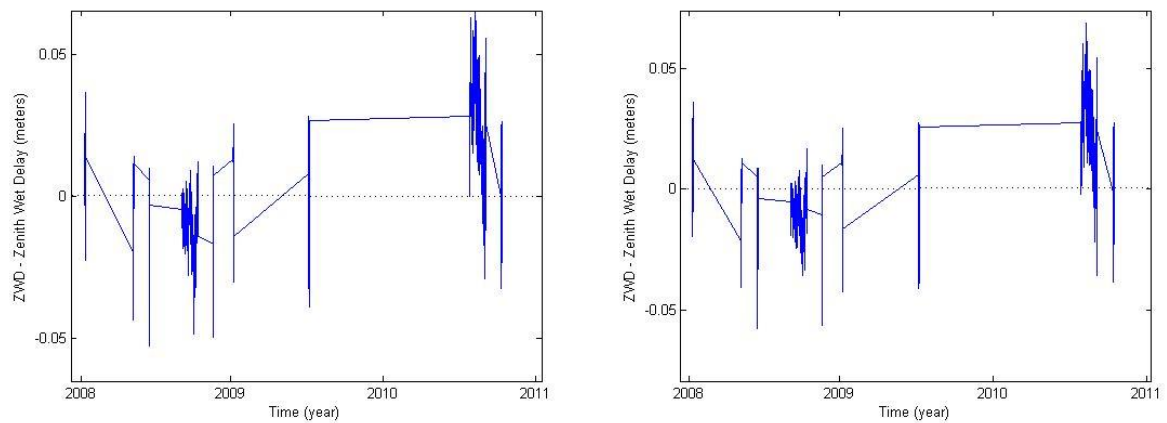


Figure 39: Nyborg station comparison plot with ECMWF (left), Comparison with RCA (right). Dotted line is the zero axes

OVT0:

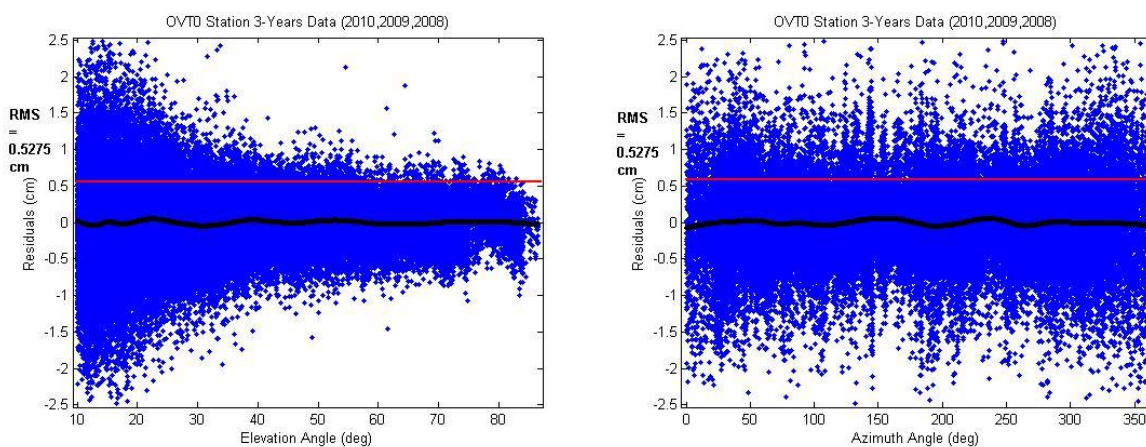


Figure 23: Övertorneå station Residual plot as an angle of Elevation angle (left) and as an angle of Azimuth angle (right). Black line is the trend; red line is the root mean square

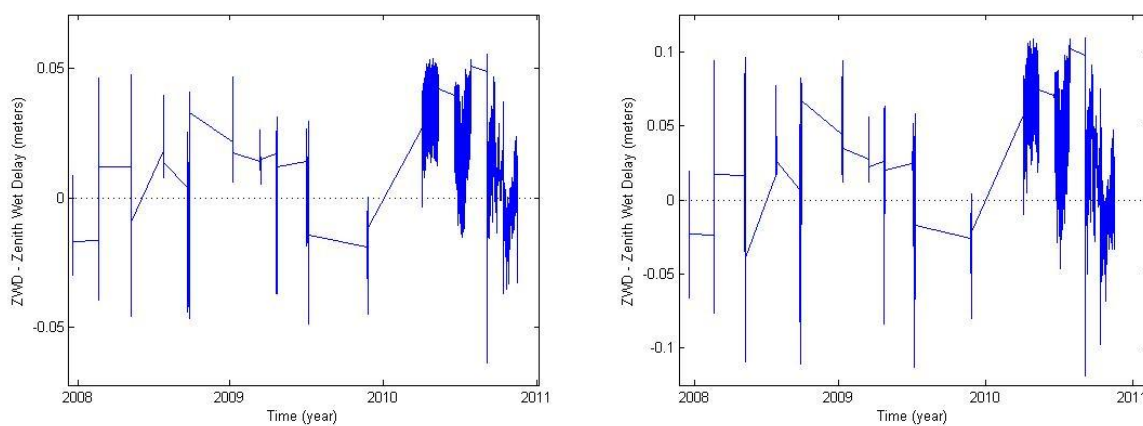


Figure 40: Övertorneå stations comparison plot with ECMWF (left), Comparison with RCA (right). Dotted line is the zero axes

OXE0:

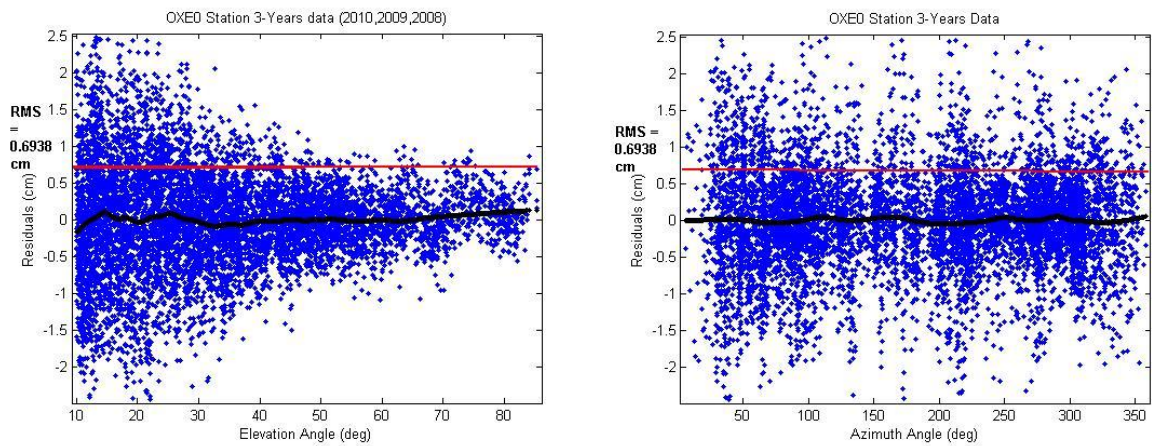


Figure 26: Oxelösund station Residual plot as an angle of Elevation angle (left) and as an angle of Azimuth angle (right). Black line is the trend; red line is the root mean square

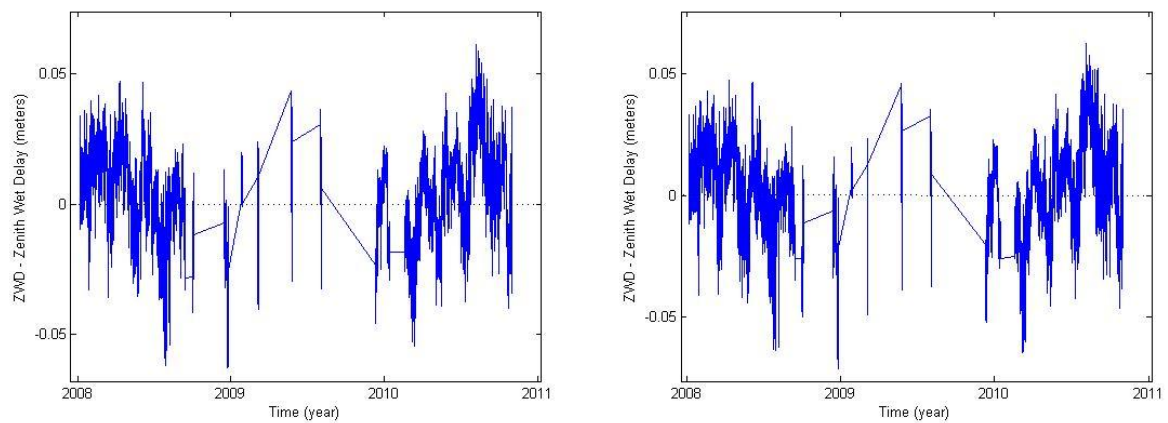


Figure 41: Oxelösund station comparison plot with ECMWF (left), Comparison with RCA (right). Dotted line is the zero axes

STA0:

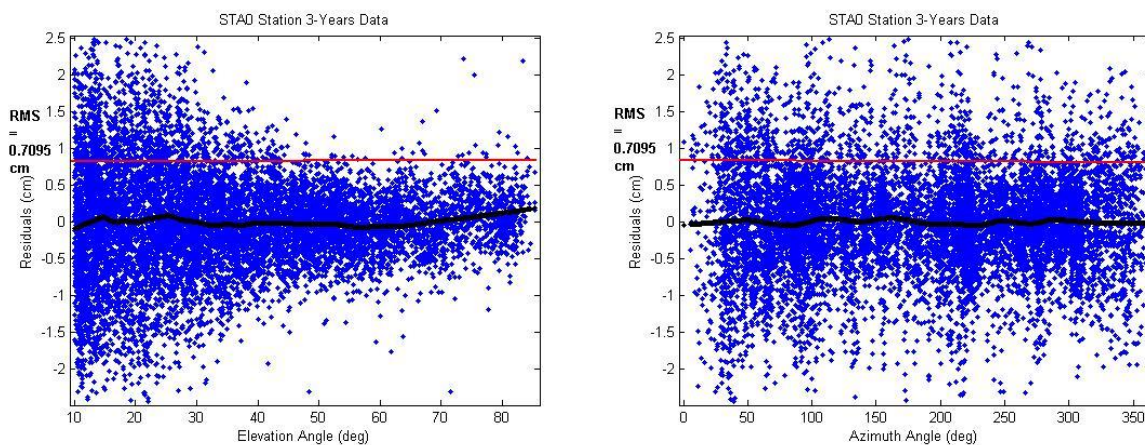


Figure 29: Stavsnäs station Residual plot as an angle of Elevation angle (left) and as an angle of Azimuth angle (right). Black line is the trend; red line is the root mean square

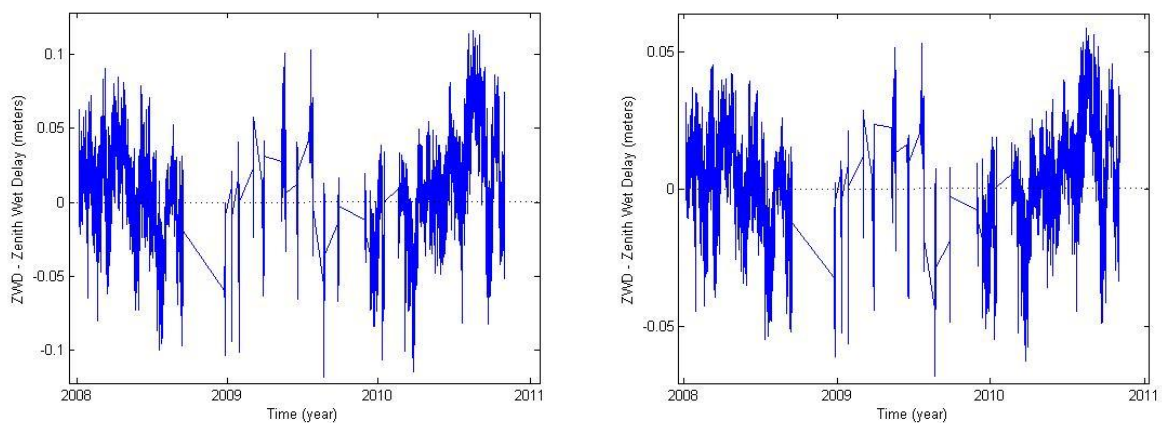


Figure 42: Stavsnäs station comparison plot with ECMWF (left), Comparison with RCA (right). Dotted line is the zero axes

VASO:

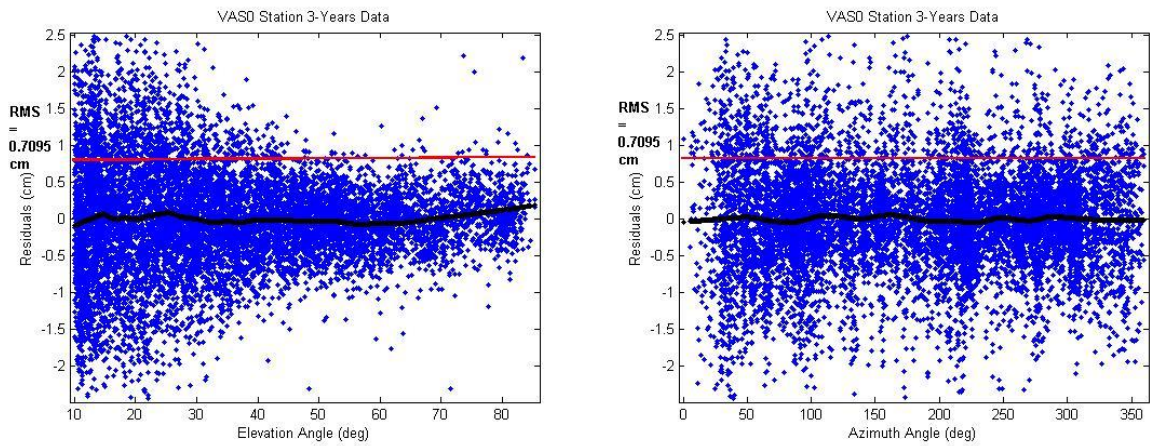


Figure 32: Västerås station Residual plot as an angle of Elevation angle (left) and as an angle of Azimuth angle (right). Black line is the trend; red line is the root mean square

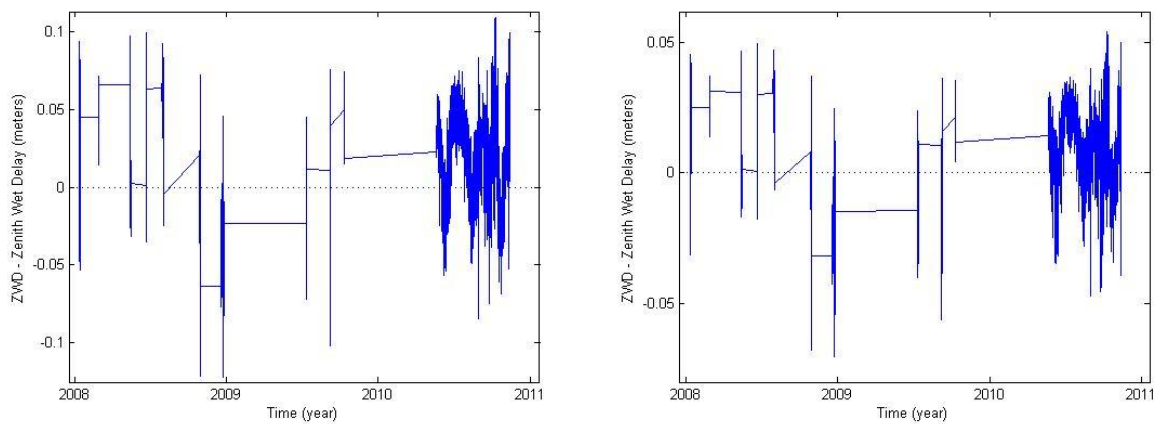


Figure 43: Västerås station comparison plot with ECMWF (left), Comparison with RCA (right). Dotted line is the zero axes

VINO:

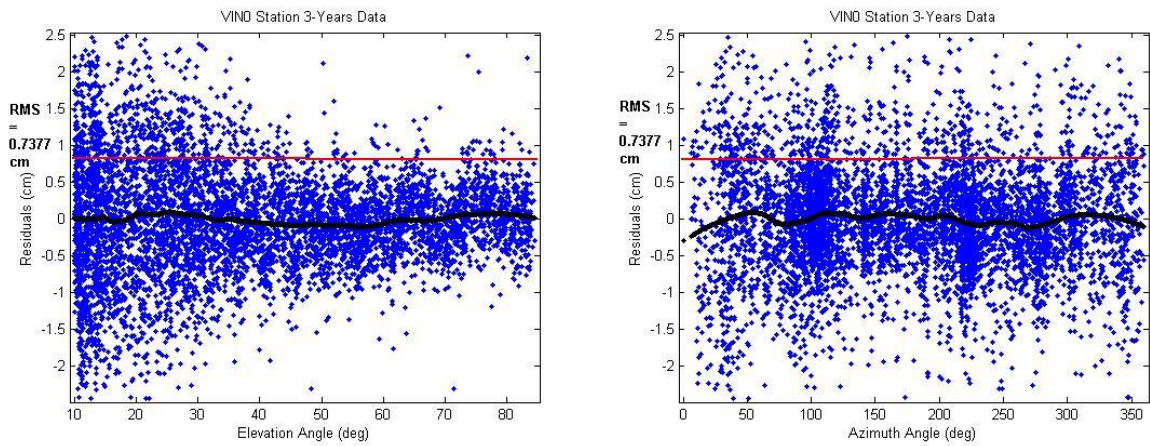


Figure 35: VindelIn station Residual plot as an angle of Elevation angle (left) and as an angle of Azimuth angle (right). Black line is the trend; red line is the root mean square

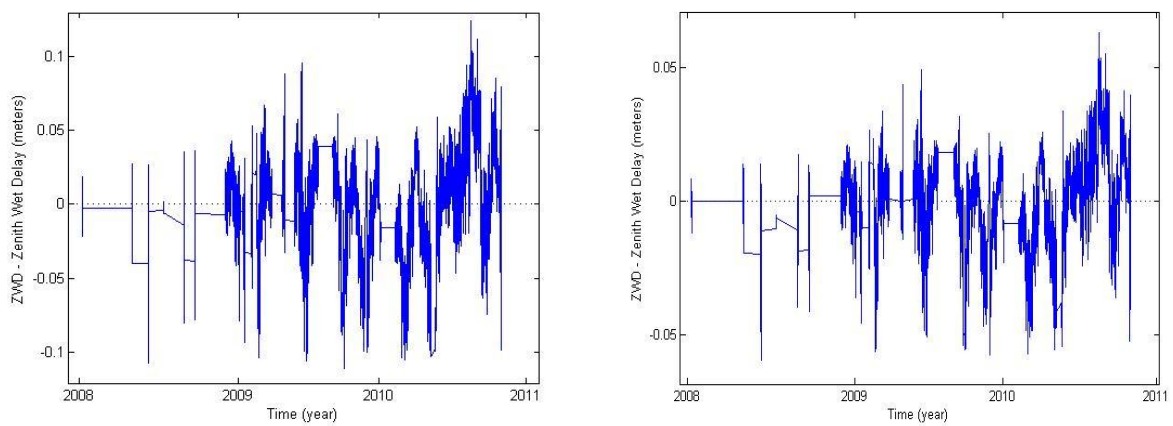


Figure 44: VindelIn station comparison plot with ECMWF (left), Comparison with RCA (right). Dotted line is the zero axes